

# Maximum Norm Error Estimation for the Finite Element Solution to Partial Differential Equations

Shirley Mae Galindo

Doctoral Program in Fundamental Sciences  
Graduate School of Science and Technology  
Niigata University

August 2022

## ACKNOWLEDGEMENT

I want to extend a sincere and heartfelt obligation towards all the personages without whom the completion of the project was not possible.

I express my profound gratitude and deep regard to Prof. Xuefeng LIU, for his guidance, valuable feedback, and constant encouragement throughout the project. His expertise and patience has helped me overcome the hardest of hurdles.

I am highly indebted to Prof. Koichiro IKE, whose intuitiveness and insight has been invaluable to the progression of this project, allowing it to mature into the project it is today.

I am immensely grateful to Prof. Tamaki TANAKA and Prof. Syuuji YAMADA for lending their expertise in the development of the study.

I am also grateful to the Niigata University Graduate School of Science and Technology Department of Mathematics of the Faculty of Science for allowing me to do this project and providing all the required facilities.

**Shirley Mae Galindo**

[August 2022]

# ABSTRACT

The Lagrange interpolation is one of the most used interpolation types to approximate functions. Its interpolation error has been estimated under various norms and is a widely explored topic in numerical analysis. Error estimation for the approximation of functions greatly affects the development of numerical solutions to partial differential equations. For example, the maximum norm of the interpolation error influences the discretization error of the finite element method (FEM) solution.

In this research, we consider the  $L^\infty$ -norm estimation for the linear Lagrange interpolation over a triangle element  $K$  by using the  $H^2$ -seminorm of the objective function, that is, to obtain the explicit estimate of the constant satisfying

$$\|u - \Pi^L u\|_{\infty, K} \leq C^L(K) |u|_{2, K}, \forall u \in H^2(K).$$

Here,  $C^L(K)$  is the interpolation error constant to be evaluated explicitly. Waldron (1998) estimated the maximum norm of the Lagrange interpolation error in terms of the maximum of the second derivative of the objective function, i.e.,  $\|u^{(2)}\|_{\infty, K}$ . Since the  $H^2$ -seminorm of the function requires less function regularity than  $\|u^{(2)}\|_{\infty, K}$  norm, the result of this research has more application.

For triangle element  $K$  of general shape, a formula to give an estimate of the interpolation error constant  $C^L(K)$  is obtained through theoretical analysis. The theoretical estimation leads to a raw bound that works well for triangle of arbitrary shapes. Particularly, our analysis tells that the value of  $C^L(K)$  can be very large and tend to  $\infty$  if the triangle element tends to degenerate to a 1D segment.

An algorithm for the optimal estimation for  $C^L(K)$  is also proposed, which ex-

tends the technique of eigenvalue estimation by Liu [17]. The objective problem is converted to a quadratic minimization problem with maximum norm constraint. To overcome the difficulty caused by the maximum norm in the constraint condition, a novel method is proposed by utilizing the orthogonality property of the interpolation associated to the Fujino-Morley FEM space and the convex-hull property of the Bernstein representation of functions in the FEM space. Specifically, for a unit right isosceles triangle  $K$ , it has been shown by rigorous computation that

$$0.40432 \leq C^L(K) \leq 0.41596.$$

Also, the maximum norm error estimation of the Lagrange interpolation has been used to estimate the local maximum error of the FEM solution to the Poisson boundary value problem. That is, given the subdomain  $\Omega' \subseteq \Omega$ , an estimator  $\xi$  is desired which satisfies

$$\|u - u_h\|_{\infty, \Omega'} \leq \xi \quad (u : \text{exact solution}, u_h : \text{FEM solution}).$$

To compute the above estimator, Fujita's method of pointwise estimation of the boundary value solution is employed, as well as the interpolation error estimation for the Lagrange interpolation.

The code is shared at <https://ganjin.online/shirley/InterpolationErrorEstimate>. Main results of this dissertation can be found in [13].

**Keywords:** Lagrange interpolation, Fujino–Morley FEM space, Bernstein polynomials, finite element method, boundary value problem, maximum norm error estimation

# Contents

<b>List of Figures</b>	<b>vii</b>
<b>List of Tables</b>	<b>ix</b>
<b>1 Introduction to Lagrange interpolation error estimation</b>	<b>1</b>
1.1 Notation for function spaces . . . . .	1
1.2 Various interpolation error estimation . . . . .	2
1.2.1 One-dimensional Lagrange interpolation . . . . .	2
1.2.2 Two-dimensional Lagrange interpolation . . . . .	5
1.3 Maximum norm error estimation . . . . .	7
<b>2 Explicit estimation of the interpolation constant</b>	<b>9</b>
2.1 Trace theorem . . . . .	9

2.2	The case for a unit right isosceles triangle . . . . .	13
2.3	Dependence of the constant on the shape of $K$ . . . . .	14
<b>3</b>	<b>Solution to optimization problems involving maximum norm</b>	<b>18</b>
3.1	Optimization problem with maximum norm constraint . . . . .	19
3.2	Lower bound for $\lambda$ . . . . .	21
3.2.1	Estimation of $C_h^{FM}$ . . . . .	22
3.2.2	Estimation of $\lambda_h$ . . . . .	23
3.3	Lower bound for the interpolation constant . . . . .	29
3.4	Numerical results . . . . .	31
3.4.1	Computed interpolation constants for various triangles . . . . .	31
3.5	Rigorous result using interval arithmetic . . . . .	32
<b>4</b>	<b>Application to partial differential equations</b>	<b>35</b>
4.1	Local maximum norm error estimation . . . . .	36
4.2	Numerical results and discussion . . . . .	38
4.2.1	Order of convergence . . . . .	41
<b>5</b>	<b>Conclusion</b>	<b>45</b>

A Useful inequalities	47
B Transformation from Bernstein coefficients to Fujino–Morley coefficients	51
C Algorithm for interpolation error constant estimation	57
D Fujita’s method of pointwise estimation	64
Bibliography	67

# List of Figures

1.1	A linear Lagrange interpolation function $\Pi^L u$ defined on a triangle $K$ ([13]). . . . .	5
1.2	Configuration of triangle $K_{\alpha,\theta,h}$ ([13]). . . . .	8
2.1	A triangle $K$ with base $e$ and height $H_K$ ([13]). . . . .	10
2.2	A subtriangle $\tilde{K}$ in a triangle $K$ ([13]). . . . .	11
2.3	A right isosceles triangle $K_{1,\frac{\pi}{2},h}$ ([13]). . . . .	13
2.4	A triangle $K_{\alpha,\theta}$ with angle $\theta$ close to $\pi$ ([13]). . . . .	17
2.5	A right triangle $K_{\alpha,\frac{\pi}{2}}$ with one leg length close to 0 ([13]). . . . .	17
3.1	A uniform triangulation of a right isosceles triangle ([13]) . . . . .	23
3.2	Contour lines of $C^L(\alpha, \theta)$ w.r.t. vertex $p_3(x, y)$ ([13]). . . . .	30
3.3	The contour lines of the minimizer $u_h$ of (3.7) for $K_{1,\frac{\pi}{2}}$ ([13]). . . . .	32



3.4	The convergency behaviour of the upper and lower bounds of $C^L(1, \theta)$ for $\theta = \frac{\pi}{3}$ and $\frac{\pi}{2}$ ([13]). . . . .	34
4.1	The domain $\Omega$ with the subdomain of interest $\Omega'$ . . . . .	37
4.2	Domain $\Omega$ with two subdomains $\Omega'_1$ and $\Omega'_2$ . . . . .	39
B.1	The subdivision of $K$ into three subtriangles $K_1, K_2, K_3$ . . . . .	54

# List of Tables

3.1	The lower bounds for $\lambda$ through Theorem 3.2.1 and Corollary 3.2.6 ([13]). . . . .	33
3.2	The lower and upper bounds of $C^L(1, \theta)$ for triangles of different shapes ([13]). . . . .	33
4.1	Approximate pointwise values and explicit bounds obtained using Fujita's method . . . . .	40
4.2	Configurations of meshes . . . . .	43
4.3	Error terms involved in the local error estimation . . . . .	44
4.4	Relative Lagrange interpolation error . . . . .	44

# Chapter 1

## Introduction to Lagrange interpolation error estimation

In this study, we consider the error estimation for the linear Lagrange interpolation over triangle elements and provide explicit values for the error constant in the error estimation under the  $L^\infty$ -norm.

In this chapter, the existing literature for various error estimation of the Lagrange interpolation function is introduced.

### 1.1 Notation for function spaces

Let us introduce the notation for the function spaces used throughout this research. In most cases, the domain  $\Omega$  of functions is selected as a triangle element  $K$ . The standard notation is used for Sobolev function spaces  $W^{k,p}(\Omega)$ . The associated norms

and seminorms are denoted by  $\|\cdot\|_{k,p,\Omega}$  and  $|\cdot|_{k,p,\Omega}$ , respectively (see, e.g., Chapter 1 of [2] and Chapter 1 of [8], [3], [7]). Particularly, for special  $k$  and  $p$ , we use abbreviated notations as  $H^k(\Omega) = W^{k,2}(\Omega)$ ,  $|\cdot|_{k,\Omega} = |\cdot|_{k,2,\Omega}$ , and  $L^p(\Omega) = W^{0,p}(\Omega)$ . The set of polynomials over  $K$  of up to degree  $k$  is denoted by  $P_k(K)$ . The second order derivative is given by  $D^2u := (u_{xx}, u_{xy}, u_{yx}, u_{yy})$  for  $u \in H^2(\Omega)$ .

## 1.2 Various interpolation error estimation

The Lagrange interpolation, being one of the most fundamental type of interpolation, has vast studies dedicated to studying its error and efficiency.

### 1.2.1 One-dimensional Lagrange interpolation

Given  $I = (0, 1)$ , the Lagrange interpolation function  $\Pi^L u$  of  $u \in H^2(I)$  is a linear function satisfying

$$(u - \Pi^L u)(0) = (u - \Pi^L u)(1) = 0.$$

The following results are well known as optimal estimates if  $u$  is regular enough, in the sense that the right-hand sides of the inequalities are well defined:

$$\|u - \Pi^L u\|_{0,I} \leq \frac{1}{\pi^2} |u|_{2,I}, \quad |u - \Pi^L u|_{1,I} \leq \frac{1}{\pi} |u|_{2,I}, \quad \|u - \Pi^L u\|_{\infty,I} \leq \frac{1}{8} \|u^{(2)}\|_{\infty,I}$$

where  $u^{(2)}$  denotes the second derivative of  $u$ .

In particular, for the Lagrange interpolation error  $u - \Pi^L u$  defined on  $I = (0, 1)$ , by Wirtinger's inequality [10] (Lemma A.0.3),

$$\|u - \Pi^L u\|_{0,I} \leq \frac{1}{\pi} |u - \Pi^L u|_{1,I}. \quad (1.1)$$

**Proposition 1.2.1.** For  $u \in H^2(I)$ ,  $|u - \Pi^L u|_{1,I} \leq \frac{1}{\pi} |u|_{2,I}$ .

**Proposition 1.2.2.** For  $u \in H^2(I)$ ,  $\|u - \Pi^L u\|_{0,I} \leq \frac{1}{\pi^2} |u|_{2,I}$ .

*Proof.* From Wirtinger's inequality (1.1) and Proposition 1.2.1, the conclusion follows.  $\square$

**Proposition 1.2.3.** For  $u \in H^2(I)$ ,  $\|u - \Pi^L u\|_{\infty,I} \leq \frac{1}{8} \|u^{(2)}\|_{\infty,I}$ .

*Proof.* Let  $w = u - \Pi^L u$ . Then  $w(0) = w(1) = 0$ . By Extreme Value Theorem,  $w$  takes on a maximum value at say  $x_0 \in (0, 1)$ . Taking the Taylor expansion of  $w(x)$  at  $x_0$ , we have

$$w(x) = w(x_0) + w'(x_0)(x - x_0) + \frac{1}{2} w''(\xi)(x - x_0)^2 = w(x_0) + \frac{1}{2} w''(\xi)(x - x_0)^2, \quad (1.2)$$

since  $w'(x_0) = 0$ . Suppose that  $x_0 \in (0, 1/2)$ . Letting  $x = 0$  in (1.2), since  $w(x) = 0$ ,

$$|w(x_0)| = \frac{1}{2} \left(\frac{1}{2}\right)^2 |w''(\xi)| \leq \frac{1}{8} \max_{\xi \in (0,1)} |w''(\xi)|.$$

Similarly, if  $x_0 \in (1/2, 1)$ , by taking  $x = 1$ ,  $|w(x_0)| \leq \frac{1}{8} \max_{\xi \in (0,1)} |w''(\xi)|$ .

Therefore,

$$\|u - \Pi^L u\|_{\infty,I} \leq \frac{1}{8} \|u^{(2)}\|_{\infty,I}.$$

$\square$

The estimation presented above are optimal in the sense that there exist functions for which the equalities hold.

- Let  $u(x) := \sin(\pi x)$  on the interval  $(0, 1)$ . Then,  $\Pi^L u(x) = 0$ . In this case,

$$\|u - \Pi^L u\|_{0,I} = \left( \int_0^1 |\sin(\pi x)|^2 dx \right)^{1/2} = \frac{\sqrt{2}}{2}$$

while

$$|u|_{2,I} = \left( \int_0^1 |u''(x)|^2 dx \right)^{1/2} = \left( \int_0^1 |\pi^2 \sin(\pi x)|^2 dx \right)^{1/2} = \frac{\pi^2 \sqrt{2}}{2}$$

Thus,

$$\|u - \Pi^L u\|_{0,I} = \frac{1}{\pi^2} |u|_{2,I}$$

Also,

$$|u - \Pi^L u|_{1,I} = \left( \int_0^1 |\pi \cos(\pi x)|^2 dx \right)^{1/2} = \frac{\pi \sqrt{2}}{2}$$

and hence,

$$|u - \Pi^L u|_{1,I} = \frac{1}{\pi} |u|_{2,I} .$$

- Let  $u(x) := x^2$  on the interval  $(0, 1)$ . Then,  $\Pi^L u(x) = x$ . In this case,

$$\|u - \Pi^L u\|_{\infty,I} = \|x^2 - x\|_{\infty,I} = \frac{1}{4},$$

since the function  $|x^2 - x|$  attains its maximum at  $x = 0.5$  with value 0.25.

On the other hand,

$$\|u^{(2)}\|_{\infty,I} = \|u''\|_{\infty,I} = 2.$$

Therefore,

$$\|u - \Pi^L u\|_{\infty, I} = \frac{1}{8} \|u^{(2)}\|_{\infty, I}.$$

## 1.2.2 Two-dimensional Lagrange interpolation

Over a triangle  $K$  with vertices  $p_i$  ( $i = 1, 2, 3$ ), the Lagrange interpolation function  $\Pi^L u$  of  $u \in H^2(K)$  is the linear function such that (see Figure 1.1)

$$(u - \Pi^L u)(p_i) = 0, \quad \forall i = 1, 2, 3.$$

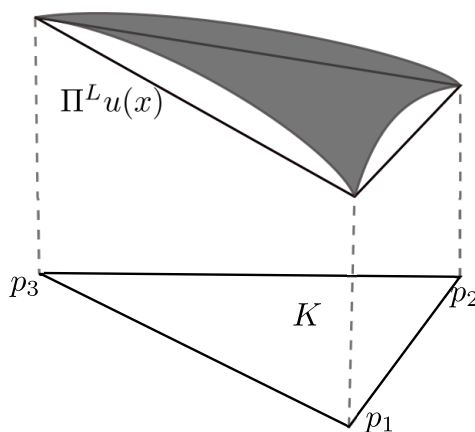


Figure 1.1: A linear Lagrange interpolation function  $\Pi^L u$  defined on a triangle  $K$  ([13]).

For the  $L^2$ -norm and  $H^1$ -seminorm error estimation of  $\Pi^L$ , one needs to estimate the interpolation error constants  $C_0$  and  $C_1$  satisfying the inequalities:

$$\|u - \Pi^L u\|_{0, K} \leq C_0(K) |u|_{2, K}, \quad |u - \Pi^L u|_{1, K} \leq C_1(K) |u|_{2, K}.$$

Let  $h$  be the medium edge length of  $K$ ,  $\theta$  the maximum angle, and  $\alpha h$  ( $0 < \alpha \leq 1$ ) the smallest edge length. Kikuchi and Liu [14, 18] obtained the bound of  $C_0$  and  $C_1$  as follows:

$$C_0(K) \leq \frac{h}{\pi} \sqrt{1 + |\cos \theta|}, \quad C_1(K) \leq 0.493h \frac{1 + \alpha^2 + \sqrt{1 + 2\alpha^2 \cos 2\theta + \alpha^4}}{\sqrt{2(1 + \alpha^2 - \sqrt{1 + 2\alpha^2 \cos 2\theta + \alpha^4})}}.$$

Another estimation for  $C_1$  was obtained by Kobayashi [15] for a triangle  $K$  with edge lengths  $A, B, C$  and area  $S$  and is given by

$$C_1(K) := \sqrt{\frac{A^2 B^2 C^2}{16S^2} - \frac{A^2 + B^2 + C^2}{30} - \frac{S^2}{5} \left( \frac{1}{A^2} + \frac{1}{B^2} + \frac{1}{C^2} \right)}.$$

The optimal estimation of constants  $C_0(K)$  and  $C_1(K)$  for a concrete  $K$  is obtained by solving corresponding eigenvalue problems with rigorous lower eigenvalue bounds; see results of [20, 23].

Waldron [24] provides the following sharp inequality for the  $L^\infty$ -norm error estimation in terms of the  $L^\infty$ -norm of second derivative of the objective function:

$$\|u - \Pi^L u\|_{\infty, K} \leq \frac{1}{2} (R^2 - d^2) \|u^{(2)}\|_{\infty, K}, \quad (1.3)$$

where  $R$  is the radius of the circumscribed circle of  $K$ ,  $d$  is the distance of the center  $c$  of the circumscribed circle from  $K$ , and  $\|u^{(2)}\|_{\infty, K}$  is defined by

$$\|u^{(2)}\|_{\infty, K} := \sup_{x \in K} \sup_{\substack{u, v \in \mathbb{R}^2 \\ \|u\| = \|v\| = 1}} |D_u D_v u(x)| = \sup_{x \in K} \sup_{\substack{\xi \in \mathbb{R}^2 \\ \|\xi\| = 1}} |D_\xi^2 u(x)|.$$



In particular, if the center  $c$  of the circumscribed circle is in  $K$ , then

$$\|u - \Pi^L u\|_{\infty, K} \leq \frac{1}{2} R^2 \|u^{(2)}\|_{\infty, K}.$$

D'Azevedo and Simpson [9] provided results for the  $L^\infty$ -norm of the interpolation error for quadratic polynomials  $f$ . In [22], Shewchuk discussed extensively the  $L^\infty$ -norm for both  $f - \Pi^L f$  and  $\nabla(f - \Pi^L f)$  for both triangular and tetrahedral elements. On the other hand, the relation between the geometric aspect ratio of the triangle element to the interpolation error was examined by Cao [4].

### 1.3 Maximum norm error estimation

In this research, we consider the  $L^\infty$ -norm error estimation for the Lagrange interpolation over triangle element  $K$  by using the  $H^2$ -seminorm of the objective function. Specifically, this study aims to evaluate explicitly the interpolation error constant  $C^L(K)$  satisfying the inequality

$$\|u - \Pi^L u\|_{\infty, K} \leq C^L(K) |u|_{2, K}, \quad \forall u \in H^2(K). \quad (1.4)$$

Note that since  $W^{2, \infty}(K) \subseteq H^2(K)$ , the inequality (1.4) is more general than Waldron's result (1.3).

Given a triangle  $K$ , denote each vertex by  $p_i$  ( $i = 1, 2, 3$ ) and the largest edge length by  $h_K$ ; see Figure 1.2. We follow the notation introduced by Liu and Kikuchi [18] to configure a general triangle with geometric parameters. Let  $h, \alpha$  and  $\theta$  be

positive constants such that

$$h > 0, \quad 0 < \alpha \leq 1, \quad \left(\frac{\pi}{3} \leq\right) \cos^{-1} \left(\frac{\alpha}{2}\right) \leq \theta < \pi.$$

Define a triangle  $K_{\alpha,\theta,h}$  with three vertices  $p_1(0, 0)$ ,  $p_2(h, 0)$  and  $p_3(\alpha h \cos \theta, \alpha h \sin \theta)$ .

Note that  $h \leq h_K$ . In case of  $h = 1$ , the notation  $K_{\alpha,\theta,1}$  is abbreviated as  $K_{\alpha,\theta}$ .

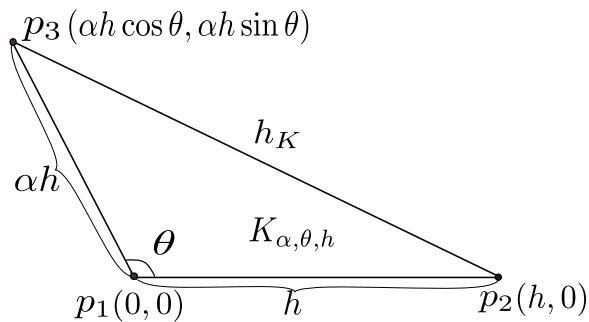


Figure 1.2: Configuration of triangle  $K_{\alpha,\theta,h}$  ([13]).

With the above configuration of the triangle  $K_{\alpha,\theta,h}$ , the optimal constant  $C^L(K)$  in (1.4) can be defined as follows:

$$C^L(\alpha, \theta, h) := \sup_{u \in H^2(K_{\alpha,\theta,h})} \frac{\|u - \Pi^L u\|_{\infty, K_{\alpha,\theta,h}}}{|u|_{2, K_{\alpha,\theta,h}}}. \quad (1.5)$$

By scaling of the triangle element, it is easy to confirm that  $C^L(\alpha, \theta, h) = hC^L(\alpha, \theta, 1)$ .

The main results presented in this dissertation can be found in [13].

# Chapter 2

## Explicit estimation of the interpolation constant

In this chapter, the raw estimation of the desired constant is obtained through theoretical analysis.

### 2.1 Trace theorem

First, let us quote a lemma about the trace theorem, which gives estimation for the integral over edge of a triangle element. For convenience, the proof is shown in a concise way; refer to e.g. [1, 5, 25] for more detailed discussion.

**Lemma 2.1.1** (Trace theorem). *Let  $e$  be one of the edges of triangle  $K$ ; see Figure*

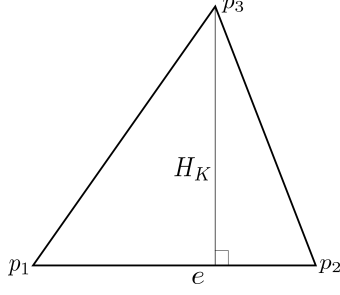


Figure 2.1: A triangle  $K$  with base  $e$  and height  $H_K$  ([13]).

2.1. Given  $w \in H^1(K)$ , we have the following estimation:

$$\|w\|_{0,e}^2 \leq \frac{|e|}{|K|} \left\{ \|w\|_{0,K}^2 + h_K \|w\|_{0,K} |w|_{1,K} \right\}.$$

*Proof.* For any  $w \in H^1(K)$ , the Green theorem leads to

$$\int_K ((x, y) - p_3) \cdot \nabla(w^2) dK = \int_{\partial K} ((x, y) - p_3) \cdot \vec{n} w^2 ds - \int_K 2w^2 dK.$$

Here,  $\vec{n}$  is the unit outer normal direction on the boundary of  $K$ . Note that

$$((x, y) - p_3) \cdot \vec{n} = \begin{cases} 0 & \text{on } p_1p_3, p_2p_3, \\ H_K & \text{on } e, \end{cases}$$

where  $H_K$  is the height of the triangle with base as  $e$ . Thus,

$$\begin{aligned}
H_K \int_e w^2 ds &= \int_K 2w^2 dK + \int_K ((x, y) - p_3) \cdot \nabla(w^2) dK \\
&\leq \int_K 2w^2 dK + 2h_K \int_K w |\nabla w| dK \\
&\leq 2 \|w\|_{0,K}^2 + 2h_K \|w\|_{0,K} \|\nabla w\|_{0,K}.
\end{aligned}$$

The conclusion follows since  $2|K| = |e|H_K$ , where  $K$  denotes the area of  $K$ .  $\square$

Using the trace theorem, the next lemma shows the pointwise estimation of the interpolation error.

**Lemma 2.1.2.** *Given  $u \in H^2(K)$ , for any point  $\mathbf{x}_0 \in K$ , we have*

$$|(u - \Pi^L u)(\mathbf{x}_0)| \leq \frac{\sqrt{2} |p_1 \mathbf{x}_0|}{\sqrt{H_{\tilde{K}}}} \left( h_K |u - \Pi^L u|_{1,K} |u|_{2,K} + |u - \Pi^L u|_{1,K}^2 \right)^{\frac{1}{2}},$$

where  $h_K$  is the longest edge length of  $K$ , and  $H_{\tilde{K}}$  is the height of the subtriangle  $\tilde{K} = p_1 \mathbf{x}_0 p_3$  with respect to the base  $\tilde{e} = p_1 \mathbf{x}_0$  (see Figure 2.2).

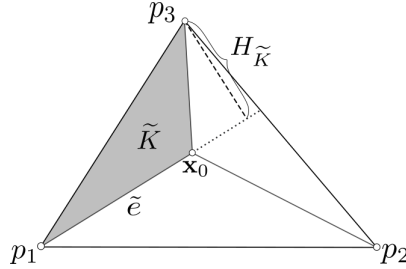


Figure 2.2: A subtriangle  $\tilde{K}$  in a triangle  $K$  ([13]).

*Proof.* Let  $g = u - \Pi^L u$  and  $t$  be the direction along edge  $p_1 \mathbf{x}_0$ . In Lemma 2.1.1, by

taking  $w := \frac{\partial g}{\partial t}$ , we have

$$\left\| \frac{\partial g}{\partial t} \right\|_{0, \tilde{e}}^2 \leq \frac{|\tilde{e}|}{|\tilde{K}|} \left( \|w\|_{0, \tilde{K}}^2 + h_{\tilde{K}} \|w\|_{0, \tilde{K}} |w|_{1, \tilde{K}} \right) \leq \frac{|\tilde{e}|}{|\tilde{K}|} \left( |g|_{1, \tilde{K}}^2 + h_{\tilde{K}} |g|_{1, \tilde{K}} |g|_{2, \tilde{K}} \right).$$

Taking the Taylor expansion of  $g$  on the segment  $\tilde{e}$  and noting that  $g(p_1) = 0$ ,

$$\begin{aligned} |g(\mathbf{x}_0)| &= \left| \int_{p_1 \mathbf{x}_0} \frac{\partial g}{\partial t} dt + g(p_1) \right| \leq \sqrt{|p_1 \mathbf{x}_0|} \cdot \left\| \frac{\partial g}{\partial t} \right\|_{0, \tilde{e}} \\ &\leq \frac{|p_1 \mathbf{x}_0|}{\sqrt{|\tilde{K}|}} \left( h_K |g|_{1, \tilde{K}} |g|_{2, \tilde{K}} + |g|_{1, \tilde{K}}^2 \right)^{\frac{1}{2}} \\ &\leq \frac{\sqrt{2} |p_1 \mathbf{x}_0|}{\sqrt{H_{\tilde{K}}}} \left( h_K |g|_{1, K} |g|_{2, K} + |g|_{1, K}^2 \right)^{\frac{1}{2}}. \end{aligned}$$

The conclusion follows.  $\square$

Liu and Kikuchi [18] considered the estimation of the constant  $C_1(\alpha, \theta)$  for different types of triangles  $K = K_{\alpha, \theta}$  such that

$$|u - \Pi^L u|_{1, K} \leq C_1(\alpha, \theta) h |u|_{2, K}, \quad \forall u \in H^2(K), \quad (2.1)$$

where  $h$  is the medium length of  $K$ . The constant  $C_1(\alpha, \theta)$  is used to give a bound for  $C^L(K)$  as shown in the lemma below.

**Lemma 2.1.3.** *Given  $u \in H^2(K)$ , for any point  $\mathbf{x}_0 \in K$ , we have*

$$|(u - \Pi^L u)(\mathbf{x}_0)| \leq \frac{\sqrt{2} |p_1 \mathbf{x}_0|}{\sqrt{H_{\tilde{K}}}} \left( C_1(\alpha, \theta) h h_K + C_1^2(\alpha, \theta) h^2 \right)^{\frac{1}{2}} |u|_{2, K}. \quad (2.2)$$

*Proof.* The inequality follows from applying (2.1) to Lemma 2.1.2.  $\square$

## 2.2 The case for a unit right isosceles triangle

Let us consider the special case for a right isosceles triangle. In the next section, this specific bound will be used to estimate the interpolation constant for triangles of arbitrary shape.

**Proposition 2.2.1.** *For the unit right isosceles triangle  $K = K_{1, \frac{\pi}{2}, h}$ ,*

$$\|u - \Pi^L u\|_{\infty, K} \leq 1.3712h |u|_{2, K}. \quad (2.3)$$

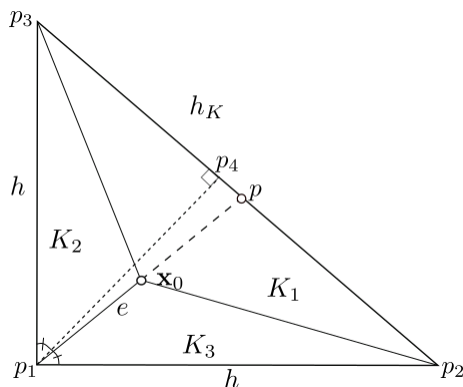


Figure 2.3: A right isosceles triangle  $K_{1, \frac{\pi}{2}, h}$  ([13]).

*Proof.* Suppose a point  $\mathbf{x}_0$  subdivides  $K$  into  $K_1, K_2, K_3$ ; see Figure 2.3. Let us consider the estimation of the term  $|p_1 \mathbf{x}_0| / H_{K_2}$ , which is required in Lemma 2.1.3. Let  $p_1 p_4$  be the height of  $K$  with base as  $p_2 p_3$ . Due to the symmetry of  $K$ , it is enough to only consider the case that  $\mathbf{x}_0 \in K$  is below the line  $p_1 p_4$ . Let  $p$  be the intersection of the extended line of  $p_1 \mathbf{x}_0$  and edge  $p_2 p_3$ . Note that  $|p_1 \mathbf{x}_0| \leq |p_1 p|$ . For

$p := (\bar{x}, \bar{y})$  on  $p_2p_4$ ,  $|p_1p| = \sqrt{\bar{x}^2 + \bar{y}^2}$ . The height of  $K_2$  with base  $p_1\mathbf{x}_0$  is given by

$$H_{K_2} = \frac{h\bar{x}}{\sqrt{\bar{x}^2 + \bar{y}^2}}.$$

Then, since  $\bar{y} = h - \bar{x}$ ,

$$\frac{|p_1p|}{H_{K_2}} = \frac{2\bar{x}^2 - 2h\bar{x} + h^2}{h\bar{x}}.$$

The above quantity takes its maximum value at  $p = (\frac{h}{2}, \frac{h}{2})$  and  $p = (h, 0)$ , and its maximum value is 1. Thus, for any  $p$  on  $p_2p_4$ ,  $|p_1p|/H_{K_2} \leq 1$ . From [18],  $C_1(1, \frac{\pi}{2}) \leq 0.49293$ . Since  $h_K = \sqrt{2}h$ , by inequality (2.2),

$$|(u - \Pi^L u)(\mathbf{x}_0)| \leq \sqrt{2} \left[ (0.49293)\sqrt{2} + 0.49293^2 \right]^{\frac{1}{2}} h |u|_{2,K} \leq 1.3712h |u|_{2,K}.$$

□

## 2.3 Dependence of the constant on the shape of $K$

Here, we consider the variation of the interpolation constant when a reference triangle, i.e., the right isosceles triangle, is transformed to a general triangle.

**Theorem 2.3.1.** *For a general element  $K_{\alpha,\theta}$ , the following estimation for constant  $C^L(\alpha, \theta)$  holds:*

$$C^L(\alpha, \theta) \leq \frac{v_+(\alpha, \theta)}{2\sqrt{\alpha \sin \theta}} C^L\left(1, \frac{\pi}{2}\right), \quad (2.4)$$



where  $v_+(\alpha, \theta) = 1 + \alpha^2 + \sqrt{1 + 2\alpha^2 \cos 2\theta + \alpha^4}$ .

*Proof.* Let us consider the affine transformation between  $x = (x_1, x_2) \in K_{\alpha, \theta}$  and  $\xi = (\xi_1, \xi_2) \in K_{1, \frac{\pi}{2}}$ :

$$\xi_1 = x_1 - \frac{x_2}{\tan \theta}, \quad \xi_2 = \frac{x_2}{\alpha \sin \theta}, \quad \text{or} \quad x_1 = \xi_1 + \alpha \xi_2 \cos \theta, \quad x_2 = \alpha \xi_2 \sin \theta.$$

Given  $\tilde{v}(\xi)$  over  $K_{1, \frac{\pi}{2}}$ , define  $v(x)$  over  $K_{\alpha, \theta}$  by  $v(x_1, x_2) = \tilde{v}(\xi_1, \xi_2)$ . Thus,

$$\|v\|_{\infty, K_{\alpha, \theta}} = \|\tilde{v}\|_{\infty, K_{1, \frac{\pi}{2}}}.$$

The estimation for the variation of  $H^2$ -seminorm in Theorem 1 of [18] tells that

$$|v|_{2, K_{\alpha, \theta}} \geq \frac{2\sqrt{\alpha \sin \theta}}{v_+(\alpha, \theta)} |\tilde{v}|_{2, K_{1, \frac{\pi}{2}}}.$$

Thus, we draw the conclusion from the definition of constant  $C^L(\alpha, \theta)$  in (1.5).  $\square$

**Lemma 2.3.2.** *For shape-regular triangles,  $C^L(\alpha, \theta)$  is bounded. Here, by “shape-regular triangles” it means that for certain positive quantity  $\delta$ , the minimal inner angle of each triangle, denoted by  $\theta_{min}$ , the inequality  $\theta_{min} \geq \delta$  holds.*

*Proof.* Suppose that there exists  $\delta > 0$  such that the minimum inner angle of the triangle, denoted by  $\theta_{min}$ , satisfies the inequality  $(\theta >) \theta_{min} \geq \delta$ . Note that  $\theta \geq \frac{\pi}{3}$ ,  $\theta + \theta_{min} < \pi$ ,

$$\sin \delta \leq \sin \theta_{min} \leq \sin \theta \quad \text{and} \quad \cos 2\theta \leq \cos 2\theta_{min} \leq \cos 2\delta.$$

Thus,

$$\frac{1 + \alpha^2 + \sqrt{1 + 2\alpha^2 \cos 2\theta + \alpha^4}}{2\sqrt{\alpha \sin \theta}} \leq \frac{1 + \alpha^2 + \sqrt{1 + 2\alpha^2 \cos 2\delta + \alpha^4}}{2\sqrt{\alpha \sin \delta}}.$$

Since  $C^L(1, \frac{\pi}{2})$  has a finite value, we draw the conclusion from the estimation (2.4).  $\square$

*Remark 2.3.3.* By using the raw bound of  $C^L(1, \frac{\pi}{2}) \leq 1.3712h$  in (2.3), an explicit but raw bound of  $C^L(\alpha, \theta)$  is available. Later, with a sharp and rigorous estimation of  $C^L(1, \frac{\pi}{2})$  based on numerical approach, the bound can be improved as

$$C^L(\alpha, \theta, h) \leq 0.41596h \frac{v_+(\alpha, \theta)}{2\sqrt{\alpha \sin \theta}}. \quad (2.5)$$

*Remark 2.3.4.* Here are two remarks on the asymptotic behavior of the constant when the triangle degenerates to a segment.

1. Suppose the maximum inner angle  $\theta$  of  $K_{\alpha, \theta}$  is close to  $\pi$ ; see Figure 2.4. Let  $u(x, y) := x^2 + y^2$ . Then,  $\Pi^L u(x, y) = x + ((\alpha - \cos \theta) / \sin \theta)y$  and

$$\|u - \Pi^L u\|_{\infty, K_{\alpha, \theta}} = (2\alpha \cos \theta - \alpha^2 - 1)/4, \quad |u|_{2, K_{\alpha, \theta}} = 2\sqrt{\alpha \sin \theta}.$$

Thus, we have a lower bound of  $C^L(\alpha, \theta)$  as follows,

$$C^L(\alpha, \theta) \geq \frac{2\alpha \cos \theta - \alpha^2 - 1}{8\sqrt{\alpha \sin \theta}}.$$

In this case,  $C^L(\alpha, \theta)$  diverges to  $\infty$  as  $\theta$  tends to  $\pi$ .

2. For triangle  $K_{\alpha, \frac{\pi}{2}}$  shown in Figure 2.5, let  $u(x, y) := |(x, y) - p_4|^2$ , where  $p_4$  is

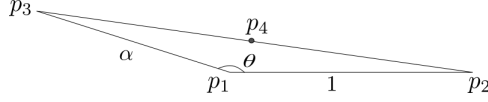


Figure 2.4: A triangle  $K_{\alpha, \theta}$  with angle  $\theta$  close to  $\pi$  ([13]).

the midpoint of the edge  $p_2 p_3$ . Then,  $\Pi^L u = (\alpha^2 + 1)/4$  and

$$\|u - \Pi^L u\|_{\infty, K_{\alpha, \frac{\pi}{2}}} = (\alpha^2 + 1)/4, \quad |u|_{2, K_{\alpha, \frac{\pi}{2}}} = 2\sqrt{\alpha}.$$

Thus,

$$\frac{\|u - \Pi^L u\|_{\infty, K_{\alpha, \frac{\pi}{2}}}}{|u|_{2, K_{\alpha, \frac{\pi}{2}}}} = \frac{\alpha^2 + 1}{8\sqrt{\alpha}} \left( \leq C^L \left( \alpha, \frac{\pi}{2} \right) \right).$$

In case that  $\alpha \rightarrow 0$ , although the maximum inner angle is invariant, the interpolation error constant  $C^L \left( \alpha, \frac{\pi}{2} \right)$  tends to  $\infty$ .

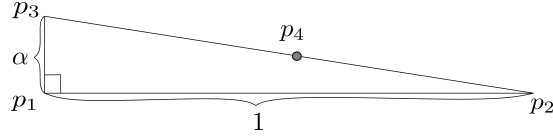


Figure 2.5: A right triangle  $K_{\alpha, \frac{\pi}{2}}$  with one leg length close to 0 ([13]).

## Chapter 3

# Solution to optimization problems involving maximum norm

In the previous chapter, the bounds for the interpolation constant obtained through theoretical analysis are applicable to triangles of any shape. However, such bounds only provide raw bounds for the objective constant. In this chapter, we propose a numerical algorithm to obtain the optimal estimation of the constant  $C^L(K)$  for various triangles by solving optimization problems with constraint involving the maximum norm.

### 3.1 Optimization problem with maximum norm constraint

Let us formulate the optimization problem to determine the interpolation error constant. The function spaces and finite element spaces along with their associated norms and seminorms that will be used throughout the chapter are first introduced below.

Let  $V^L(K) := \{u \in H^2(K) \mid u(p_i) = 0 \ (i = 1, 2, 3)\}$ . Also, let  $\mathcal{T}^h$  be a triangulation of  $K$  and define the space

$$V_h^{FM}(K) := \left\{ v \mid v|_{K_h} \in P_2(K_h), \forall K_h \in \mathcal{T}^h; v(p_i) = 0 \ (i = 1, 2, 3); v \text{ is continuous at the nodes; } \int_e \left( \frac{\partial v}{\partial \vec{n}} \Big|_{K_h} - \frac{\partial v}{\partial \vec{n}} \Big|_{K'_h} \right) ds = 0 \text{ for each } e = K_h \cap K_{h'} \right\}.$$

For  $u_h, v_h \in V_h^{FM}(K)$ , define the discretized  $H^2$ -inner product and seminorm by

$$\langle u_h, v_h \rangle_h := \sum_{K_h \in \mathcal{T}^h} \int_{K_h} D^2 u_h|_{K_h} \cdot D^2 v_h|_{K_h} \, dK_h, \quad |u_h|_{2,K} := \sqrt{\langle u_h, u_h \rangle_h}.$$

Let us define the two quantities over the triangle  $K$ :

$$\lambda(K) := \inf_{u \in V^L(K)} \frac{|u|_{2,K}^2}{\|u\|_{\infty,K}^2}, \quad \lambda_h(K) := \min_{u_h \in V_h^{FM}(K)} \frac{|u_h|_{2,K}^2}{\|u_h\|_{\infty,K}^2}. \quad (3.1)$$

*Remark 3.1.1.* By the definition of the optimal value for  $C^L(K)$ ,

$$C^L(K) = \sqrt{\lambda(K)}^{-1}.$$

Hence, a lower bound for  $\lambda$  will be used to obtain an upper bound for the objective interpolation error constant  $C^L(K)$ .

**Fujino–Morley interpolation** Given  $u \in H^2(K)$ , the Fujino–Morley interpolation  $\Pi_h^{FM}u$  is a function satisfying

$$\Pi_h^{FM}u \in V_h^{FM}(K); \quad \Pi_h^{FM}u|_{K_h} \in P_2(K_h), \quad \forall K_h \in \mathcal{T}^h,$$

and at the vertices  $p_i$  and edges  $e_i$  of  $K$ ,

$$(u - \Pi_h^{FM}u)(p_i) = 0, \quad \int_{e_i} \frac{\partial}{\partial n} (u - \Pi_h^{FM}u) ds = 0 \quad (i = 1, 2, 3).$$

The Fujino–Morley interpolation has the property that (see, e.g., [20, 23])

$$\langle u - \Pi_h^{FM}u, v_h \rangle_h = 0, \quad \forall v_h \in V_h^{FM}(K). \quad (3.2)$$

Let  $V(h) := \{u + u_h \mid u \in V^L(K), u_h \in V_h^{FM}(K)\}$ . Note that the Fujino–Morley interpolation is just the projection  $P_h : V(h) \rightarrow V_h^{FM}(K)$  with respect to the inner product  $\langle \cdot, \cdot \rangle_h$ .

Let  $C_h^{FM}$  be a quantity that makes the following inequality hold.

$$\|u - \Pi_h^{FM}u\|_{\infty, K} \leq C_h^{FM} |u - \Pi_h^{FM}u|_{2, K}, \quad \forall u \in V^L(K). \quad (3.3)$$

## 3.2 Lower bound for $\lambda$

The next theorem provides an explicit lower bound of  $\lambda$ , which was inspired by the idea of [17] for the lower bounds of eigenvalue problems.

**Theorem 3.2.1.** *With the quantity  $C_h^{FM}$ , we have a lower bound of  $\lambda(K)$  as follows.*

$$\lambda(K) \geq \frac{\lambda_h}{1 + (C_h^{FM})^2 \lambda_h} . \quad (3.4)$$

*Proof.* For any  $u \in V^L(K)$ , since  $\Pi_h^{FM} u \in V_h^{FM}(K)$ ,  $|\Pi_h^{FM} u|_{2,K} \geq \sqrt{\lambda_h} \|\Pi_h^{FM} u\|_{\infty,K}$ .

Applying the inequality (3.3), we have

$$\begin{aligned} \|u\|_{\infty,K} &= \|\Pi_h^{FM} u + u - \Pi_h^{FM} u\|_{\infty,K} \\ &\leq \|\Pi_h^{FM} u\|_{\infty,K} + \|u - \Pi_h^{FM} u\|_{\infty,K} \\ &\leq \frac{|\Pi_h^{FM} u|_{2,K}}{\sqrt{\lambda_h}} + C_h^{FM} |u - \Pi_h^{FM} u|_{2,K} \\ &\leq \sqrt{\frac{1}{\lambda_h} + (C_h^{FM})^2} \sqrt{|\Pi_h^{FM} u|_{2,K}^2 + |u - \Pi_h^{FM} u|_{2,K}^2} . \end{aligned}$$

From the orthogonality in (3.2), we have

$$|\Pi_h^{FM} u|_{2,K}^2 + |u - \Pi_h^{FM} u|_{2,K}^2 = |u|_{2,K}^2 .$$

Thus,

$$\|u\|_{\infty,K} \leq \sqrt{\frac{1 + (C_h^{FM})^2 \lambda_h}{\lambda_h}} |u|_{2,K}, \quad \forall u \in V^L(K) .$$

From the definition of  $\lambda$  in (3.1), we draw the conclusion.  $\square$

*Remark 3.2.2.* To apply Theorem 3.2.1 for bounding  $\lambda$ , two subproblems emerge,

namely (1) to find an estimation of  $C_h^{FM}$ , and (2) to find the explicit value of  $\lambda_h$ . The next two subsections discuss these problems separately.

### 3.2.1 Estimation of $C_h^{FM}$

To have an explicit value of  $C_h^{FM}$ , we first define the quantity  $C_{res}^{FM}(K_h)$  for each element  $K_h$  in the triangulation  $\mathcal{T}^h$ :

$$C_{res}^{FM}(K_h) := \sup_{u \in H^2(K_h)} \frac{\|u - \Pi_h^{FM} u\|_{\infty, K_h}}{|u - \Pi_h^{FM} u|_{2, K_h}} = \sup_{w \in W_1} \frac{\|w\|_{\infty, K_h}}{|w|_{2, K_h}}.$$

Here,  $W_1 := \left\{ w \in H^2(K_h) \mid w(p_i) = 0, \int_{e_i} \frac{\partial w}{\partial n} ds = 0 \ (i = 1, 2, 3) \right\}$ . Noticing that  $W_1 \subseteq W_2$  for  $W_2 := \{w \in H^2(K_h) \mid w(p_i) = 0 \ (i = 1, 2, 3)\}$ , from the definition of  $C^L$  in (1.5), we have

$$C_{res}^{FM}(K_h) = \sup_{w \in W_1} \frac{\|w\|_{\infty, K_h}}{|w|_{2, K_h}} \leq \sup_{w \in W_2} \frac{\|w\|_{\infty, K_h}}{|w|_{2, K_h}} = C^L(K_h).$$

Then, the following  $C_h^{FM}$  with an upper bound makes certain (3.3) holds:

$$C_h^{FM} := \max_{K_h \in \mathcal{T}^h} C_{res}^{FM}(K_h) \left( \leq \max_{K_h \in \mathcal{T}^h} C^L(K_h) \right). \quad (3.5)$$

*Remark 3.2.3.* Let  $\mathcal{T}^h$  be a uniform triangulation of a right isosceles triangle; see a sample mesh in Figure 3.1. We choose an explicit upper bound of  $C_h^{FM}$  as  $C_h^{FM} \leq 1.3712h$ , since for each  $K_h \in \mathcal{T}^h$ ,  $C_{res}^{FM} \leq C^L(K_h) \leq 1.3712h$ , where  $h$  is the leg length of each right triangle element.



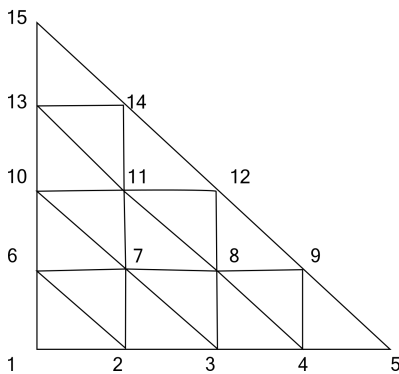


Figure 3.1: A uniform triangulation of a right isosceles triangle ([13])

### 3.2.2 Estimation of $\lambda_h$

In this part, we present a method to estimate  $\lambda_h$ , which is required in Theorem 3.2.1 for bounding  $\lambda$ . Let  $M := \text{Dim}(V_h^{FM})$ . The estimation of  $\lambda_h$  is equivalent to finding the solution to the optimization problem

$$\lambda_h = \min \mathbf{x}^T \mathbf{A} \mathbf{x}, \quad \text{subject to} \quad \left\| \sum_{i=1}^M \mathbf{x}_i \phi_i \right\|_{\infty, K} \geq 1, \quad (3.6)$$

where

- $\{\phi_i\}_{i=1, \dots, M}$  Fujino–Morley basis functions
- $\mathbf{x} \in \mathbb{R}^M$  coefficient vector for  $u_h$
- $\mathbf{A}$  matrix  $(a_{ij})_{M \times M}$ , where  $a_{ij} = \langle \phi_i, \phi_j \rangle_h$

Generally, finding the maximum of a function is not an easy task. Since the

constraint condition of the above minimization problem requires the  $L^\infty$ -norm of the function, finding its solution is also not simple.

Here, we introduce the technique to apply Bernstein polynomials and their convex-hull property to solve the problem. Strictly speaking, a new optimization problem (3.7) utilizing the Bernstein polynomials will be formulated to provide a lower bound for the solution of (3.6); refer to, e.g., [6, 11] for detailed discussion.

**Convex-hull property of Bernstein polynomials** Given a triangle  $K$ , let  $(u, v, w)$  be barycentric coordinates for a point  $x$  in  $K$ . A Bernstein polynomial  $p$  of degree  $n$  over a triangle  $K$  is defined by

$$p := \sum_{i+j+k=n} d_{i,j,k} J_{i,j,k}^{(n)}, \quad J_{i,j,k}^{(n)}(x) := \frac{n!}{i!j!k!} u^i v^j w^k.$$

Here,  $J_{i,j,k}^{(n)}(x)$  are the Bernstein basis polynomials; the coefficients  $d_{i,j,k}$  are the control points of  $p$ . Noticing that

$$J_{i,j,k}^{(n)} \geq 0, \quad \sum_{i+j+k=n} J_{i,j,k}^{(n)} = 1,$$

we can easily obtain the following convex-hull property of Bernstein polynomials:

$$\|p\|_{\infty, K} \leq \max |d_{i,j,k}|.$$

Given  $u_h \in V_h^{FM}(K)$ , for each  $K_h \in \mathcal{T}^h$ ,  $u_h|_{K_h} \in P_2(K_h)$  can be represented by the Bernstein basis polynomials of degree two. Let  $\mathbf{B}$  be the  $N \times M$  matrix that transforms the Fujino–Morley coefficients  $\mathbf{x}$  to the Bernstein coefficients  $d^B$ .

Note that  $u_h$  is regarded as a piecewise Bernstein polynomial so that its Bernstein coefficient vector  $d^B$  has the dimension  $N = 6 \times \#\{elements\}$ . The dimension of  $d^B$  can be further reduced considering the continuity of  $u_h$  at the vertices of the triangulation. However, it is difficult to utilize the constraints of  $u_h$  cross the edges to reduce the dimension  $N$ . From the convex-hull property of the Bernstein polynomials, the following inequality holds:

$$1 \leq \left\| \sum_{i=1}^M \mathbf{x}_i \phi_i \right\|_{\infty, K} \leq \|\mathbf{B}\mathbf{x}\|_{\infty}.$$

Based on this inequality, a new optimization is formulated by relaxing the constraint condition of (3.6):

$$\lambda_{h,B} = \min \mathbf{x}^T \mathbf{A}\mathbf{x}, \quad \text{subject to} \quad \|\mathbf{B}\mathbf{x}\|_{\infty} \geq 1. \quad (3.7)$$

The solution to problem (3.7) provides a lower bound for (3.6), i.e.,  $\lambda_h \geq \lambda_{h,B}$ .

Below, we propose an algorithm to solve the problem (3.7). Since  $\mathbf{A}$  is positive definite, let us consider the Cholesky decomposition of  $\mathbf{A}$ :  $\mathbf{A} = \mathbf{R}^T \mathbf{R}$ , where  $\mathbf{R}$  is an  $M \times M$  upper triangular matrix. Then, by letting  $\mathbf{y} := \mathbf{R}\mathbf{x}$  and  $\widehat{\mathbf{B}} := \mathbf{B}\mathbf{R}^{-1}$ , problem (3.7) becomes

$$\lambda_{h,B} = \min \mathbf{y}^T \mathbf{y}, \quad \text{subject to} \quad \left\| \widehat{\mathbf{B}}\mathbf{y} \right\|_{\infty} \geq 1. \quad (3.8)$$

The following lemma shows the solution for problem (3.8).

**Lemma 3.2.4.** <sup>1</sup> Let  $b_i^T$  ( $i = 1, \dots, N$ ) be the  $i$ th row of  $\widehat{\mathbf{B}}$  and  $b_{max}^T$  be a row of  $\widehat{\mathbf{B}}$

---

<sup>1</sup>Appreciation to Tamaki TANAKA and Syuuji YAMADA from Faculty of Science, Niigata University for their idea of solving this problem in an efficient way.

satisfying  $\|b_{max}\|_2 = \max_{i=1,\dots,N} \|b_i\|_2$ . Then, the optimal value of problem (3.8) is given by

$$\lambda_{h,B} = \frac{1}{\|b_{max}\|_2^2}.$$

*Proof.* Let  $S := \{\mathbf{y} \mid \|\widehat{\mathbf{B}}\mathbf{y}\|_\infty \geq 1\}$  and  $\bar{\mathbf{y}} := \|b_{max}\|_2^{-2} b_{max}$ . Then, we have  $\bar{\mathbf{y}} \in S$  because

$$\|\widehat{\mathbf{B}}\bar{\mathbf{y}}\|_\infty = \max_{i=1,\dots,N} |b_i^T \bar{\mathbf{y}}| \geq |b_{max}^T \bar{\mathbf{y}}| = 1.$$

Hence,

$$\min_{\mathbf{y} \in S} \mathbf{y}^T \mathbf{y} \leq \bar{\mathbf{y}}^T \bar{\mathbf{y}} = \frac{1}{\|b_{max}\|_2^2}. \quad (3.9)$$

For any  $\mathbf{y} \in S$ , from the Cauchy–Schwarz inequality,

$$1 \leq \max_{i=1,\dots,N} |b_i^T \mathbf{y}| \leq \max_{i=1,\dots,N} \|b_i\|_2 \|\mathbf{y}\|_2 = \|b_{max}\|_2 \|\mathbf{y}\|_2.$$

Thus,

$$\frac{1}{\|b_{max}\|_2^2} \leq \min_{\mathbf{y} \in S} \mathbf{y}^T \mathbf{y}. \quad (3.10)$$

From (3.9) and (3.10), we draw the conclusion.  $\square$

Note that the diagonal elements of  $\mathbf{B}\mathbf{A}^{-1}\mathbf{B}^T = \widehat{\mathbf{B}}\widehat{\mathbf{B}}^T$  correspond to  $\|b_i\|_2^2$  ( $i = 1, \dots, N$ ). Therefore, we can solve problem (3.7) without performing the Cholesky decomposition of  $\mathbf{A}$ , as shown by the following lemma.

**Lemma 3.2.5.** *Let  $\mathbf{D} := \mathbf{B}\mathbf{A}^{-1}\mathbf{B}^T$ . The optimal value of (3.7) is given by*

$$\lambda_{h,B} = \frac{1}{\max(\text{diag}(\mathbf{D}))},$$

where  $\text{diag}(\mathbf{D})$  is the diagonal elements of  $\mathbf{D}$ .

Theorem 3.2.1 gives a lower bound for  $\lambda$ . Since  $C^L(K) = \sqrt{\lambda(K)^{-1}}$ , this lower bound is used to obtain an upper bound for  $C^L(K)$ . Below, let us summarize the procedure to obtain a lower bound for  $\lambda$ .

**Algorithm for calculating lower bound of  $\lambda(K)$**

- a. Set up the FEM space  $V_h^{FM}(K) = \text{span}\{\phi_i\}_{i=1}^M$  over a triangulation of the triangle domain  $K$ .
- b. Assemble the global matrix  $\mathbf{A} = (a_{ij})_{M \times M}$  ( $a_{ij} = \langle \phi_i, \phi_j \rangle_h$ ) and the transformation matrix  $\mathbf{B}$  from Fujino–Morley coefficients to Bernstein coefficients.
- c. Apply Lemma 2.1.3 to obtain a raw bound for  $C_h^{FM}$ .
- d. Apply Lemma 3.2.4 or Lemma 3.2.5 to calculate  $\lambda_{h,B} (\leq \lambda_h)$ .
- e. The lower bound for  $\lambda$  is obtained through Theorem 3.2.1 by using  $\lambda_{h,B}$  and the upper bound of  $C_h^{FM}$ .

Using uniform triangulation of a domain  $K$ , a direct estimation of the lower bound for  $\lambda$  without using  $C_h^{FM}$  is available.

**Corollary 3.2.6.** *For a uniform triangulation of  $K = K_{\alpha,\theta,h}$  with  $N$  subdivisions for each side, the following holds:*

$$\lambda(K) \geq \lambda_h(1 - (1/N)^2). \tag{3.11}$$

*Proof.* Since  $(C^L(K))^2 = 1/\lambda(K)$  and each  $K_h \in \mathcal{T}^h$  is similar to  $K$ , we have,

$$\lambda(K) \geq \frac{\lambda_h}{1 + (C_h^{FM})^2 \lambda_h} \geq \frac{\lambda_h}{1 + (C^L(K_h))^2 \lambda_h} = \frac{\lambda_h}{1 + (1/N)^2 \lambda_h / \lambda(K)}.$$

The conclusion is achieved by sorting the inequality.  $\square$

*Remark 3.2.7.* Theoretically, for a refined uniform triangulation, the lower bound (3.4) using  $C_h^{FM}$  is sharper (i.e., larger) than (3.11). This fact can be confirmed by utilizing the following relation:

$$\frac{\lambda_h}{1 + (C_h^{FM})^2 \lambda_h} \geq \lambda_h(1 - (1/N)^2) \iff 1 \geq (N^2 - 1)(C_h^{FM})^2 \lambda_h. \quad (3.12)$$

For a small value of  $h = 1/N$ , we have

$$(N^2 - 1)(C_h^{FM})^2 \approx (NC_h^{FM})^2 = (C_{res}^{FM}(K_h))^2, \quad \lambda_h \approx \lambda = (C^L(K_h))^{-2}.$$

Thus, the second inequality of (3.12) holds due to  $C_{res}^{FM}(K_h) < C^L(K_h)$ . However, in practical computation, the raw estimate of  $C_{res}^{FM}(K_h)$  will cause a worse bound of  $\lambda$  than (3.11).

Using Corollary 3.2.6, the following steps are modified from the algorithm to obtain a lower bound for  $\lambda$ , without using the quantity of  $C_h^{FM}$ :

### **Revision of algorithm for calculating lower bound of $\lambda(K)$**

c\*. Apply Lemma 3.2.4 or Lemma 3.2.5 to calculate  $\lambda_{h,B}(\leq \lambda_h)$ .

d\*. Solve the lower bound for  $\lambda$  using Corollary 3.2.6 along with  $\lambda_{h,B}$ .

*Remark 3.2.8.* To compare the efficiencies of the two formulas (3.4) and (3.11), we apply them to estimate  $\lambda$  for a unit right isosceles  $K_{1, \frac{\pi}{2}}$ . By using uniform triangulation of size  $h = 1/64$ , the estimate (3.4) gives  $\lambda \geq 5.7659$  and (3.11) gives a sharper

bound as  $\lambda \geq 5.7798$ . Hence, a sharper upper bound is obtained using (3.11) and we have the following estimation:

$$\|u - \Pi^L u\|_{\infty, K_{1, \pi/2, h}} \leq 0.41596h |u|_{2, K_{1, \pi/2, h}} . \quad (3.13)$$

Recall that the theoretical result from (2.3) will yield a raw bound as  $C^L(1, \frac{\pi}{2}, h) \leq 1.3712h$ .

For a triangle  $K_{\alpha, \theta}$  with two fixed vertices  $p_1(0, 0), p_2(1, 0)$ , let us vary the vertex  $p_3(x, y)$  and calculate the approximate value of  $C^L(\alpha, \theta)$  for each position of  $p_3$ . In this case  $C^L$  can be regarded as a function with respect to the coordinate  $(x, y)$  of  $p_3$ , which is denoted by  $C^L(x, y)$ . The contour lines of  $C^L(x, y)$  are shown in Figure 3.2, where the abscissa and the ordinate denote  $x$ - and  $y$ - coordinates of  $p_3$ , respectively.

### 3.3 Lower bound for the interpolation constant

To confirm the precision of the obtained estimation for the Lagrange interpolation constant, the lower bounds of the constants are calculated. Let  $u_h$  be the function obtained by numerical computation solving the minimization problem. To obtain the lower bound, an appropriate polynomial  $f$  over  $K$  of higher degree  $d$  is selected by solving the minimization problem below:

$$\min_{f \in P_d(K)} \sum_{i=1}^n |f(p_i) - u_h(p_i)|^2 \quad (n : \#\{\text{nodes of triangulation}\})$$

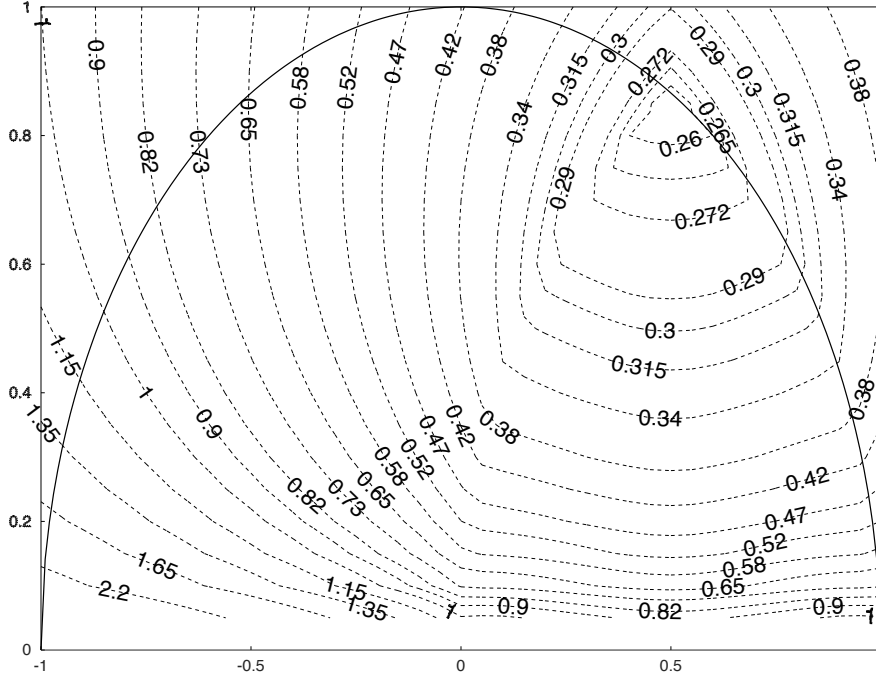


Figure 3.2: Contour lines of  $C^L(\alpha, \theta)$  w.r.t. vertex  $p_3(x, y)$  ([13]).

where  $p_i$  denote the nodes of the triangulation of  $K$ . From the definition of  $\lambda(K)$  in (3.1) and the relation  $C^L(K) = 1/\sqrt{\lambda(K)}$ , we have a lower bound of  $C^L(K)$  as follows:

$$C^L(K) \geq \frac{\|f\|_{\infty, K}}{|f|_{2, K}}.$$

*Remark 3.3.1.* For the unit right isosceles triangle  $K_{1, \frac{\pi}{2}}$ , the upper bound for the constant is obtained by solving the optimization problem through FEM with mesh size  $1/64$ . Meanwhile, the lower bound of the constant is obtained by using a polynomial of degree 9. The two-side bounds reads:

$$0.40432 \leq C^L\left(1, \frac{\pi}{2}\right) \leq 0.41596.$$



## 3.4 Numerical results

Since  $C^L(K) = \lambda^{-1/2}$ , the proposed algorithm discussed in section 3.3 gives a method of estimating the objective interpolation error constant  $C^L(K)$ .

### 3.4.1 Computed interpolation constants for various triangles

Numerical computations are performed to obtain the interpolation error constants for triangles of various shapes.

First, let us confirm the shape of the function  $u_h$  that solves the minimization problem for  $\lambda_{h,B}$  when  $K$  is the unit isosceles right triangle. The contour lines of  $u_h$  are displayed in Figure 3.3. The numerical computation tells that the maximum value of  $u_h$  happens on the midpoint of the hypotenuse of  $K$ . Note that the maximum value of  $u_h$  is around 0.95 while the maximum of its Bernstein coefficients is above 1.

Comparing the lower bounds of  $\lambda$  obtained through Theorem 3.2.1 and Corollary 3.2.6 for various triangles, Table 3.1 suggest that the values obtained using Corollary 3.2.6 gives a sharper estimate of  $\lambda$ .

Table 3.2 summarizes the results for the lower and upper bounds of the constant for different types of triangle  $K_{1,\theta}$  with the mesh size as  $h = 1/32$  and  $h = 1/64$ . The upper bounds (denoted by  $C_{ub}^L$ ) are obtained through Corollary 3.2.6, while the lower bounds (denoted by  $C_{lb}^L$ ) are obtained by using high-degree polynomials with degree denoted by  $d$ .

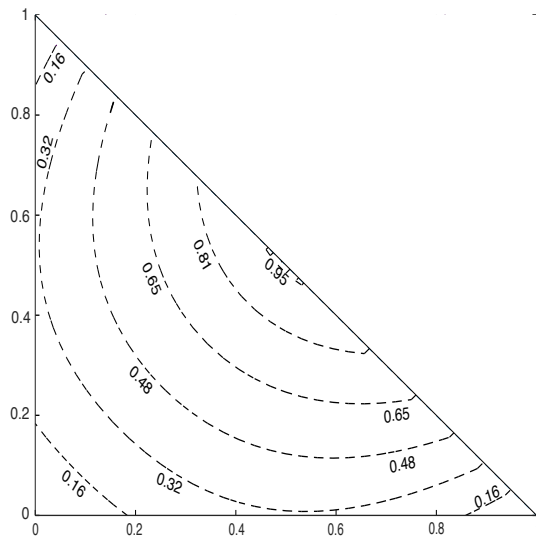


Figure 3.3: The contour lines of the minimizer  $u_h$  of (3.7) for  $K_{1, \frac{\pi}{2}}$  ([13]).

Figure 3.4 demonstrates the convergency of the upper and lower bounds of the interpolation error constant as the mesh is refined. It implies that the convergency order of upper bounds depends on the shape of the triangles. The computing code is shared at <https://ganjin.online/shirley/InterpolationErrorEstimate>. The code can be executed online under the environment provided by Ganjin online computing platform [16].

### 3.5 Rigorous result using interval arithmetic

Numerical computation with floating point-numbers involves round-off errors. To have rigorous results, we applied the interval arithmetic in assembling the matrices and evaluating the upper bound  $C_{ub}^L$  in Table 3.2. It is observed from the numerical computation results that the accumulation of round-off error in the computation is

Table 3.1: The lower bounds for  $\lambda$  through Theorem 3.2.1 and Corollary 3.2.6 ([13]).

$\theta$	$h = 1/32$			$h = 1/64$		
	$\lambda_{h,B}$	Thm. 3.1	Cor. 3.1	$\lambda_{h,B}$	Thm. 3.1	Cor. 3.1
$\pi/6$	9.8339	8.7356	9.8245	9.8925	9.5892	9.8901
$\pi/4$	13.517	12.263	13.505	13.574	13.234	13.570
$\pi/3$	15.412	14.357	15.397	15.457	15.177	15.454
$\pi/2$	5.5988	5.5418	5.5933	5.7812	5.7660	5.7799
$2\pi/3$	2.3954	2.3683	2.3930	2.5511	2.5433	2.5504
$3\pi/4$	1.5550	1.5369	1.5534	1.6768	1.6715	1.6764
$5\pi/6$	0.93778	0.92669	0.93687	1.0212	1.0179	1.0210

Table 3.2: The lower and upper bounds of  $C^L(1, \theta)$  for triangles of different shapes ([13]).

$\theta$	$h = 1/32$				$h = 1/64$			
	$d$	$C_{lb}^L$	$\lambda_{h,B}$	$C_{ub}^L$	$d$	$C_{lb}^L$	$\lambda_{h,B}$	$C_{ub}^L$
$\pi/6$	9	0.31511	9.8339	0.31904	9	0.31423	9.8925	0.31799
$\pi/4$	8	0.26777	13.517	0.27212	8	0.26753	13.574	0.27146
$\pi/3$	10	0.25182	15.412	0.25485	10	0.25209	15.457	0.25439
$\pi/2$	9	0.40432	5.5988	0.42283	9	0.40419	5.7812	0.41596
$2\pi/3$	8	0.59964	2.3954	0.64644	8	0.60079	2.5511	0.62618
$3\pi/4$	10	0.72146	1.5550	0.80233	10	0.72420	1.6768	0.77235
$5\pi/6$	8	0.92197	0.93778	1.03314	8	0.92830	1.0212	0.98968

not so large. For example, for the mesh size being  $h = 1/64$ , the matrix  $B$  has the dimension as  $24576 \times 8382$  and the rigorous estimation of  $C_{ub}^L$  in case of isosceles right triangle is given as

$$C_{ub}^L \left(1, \frac{\pi}{2}\right) \in [0.4159516728, 0.4159516793].$$

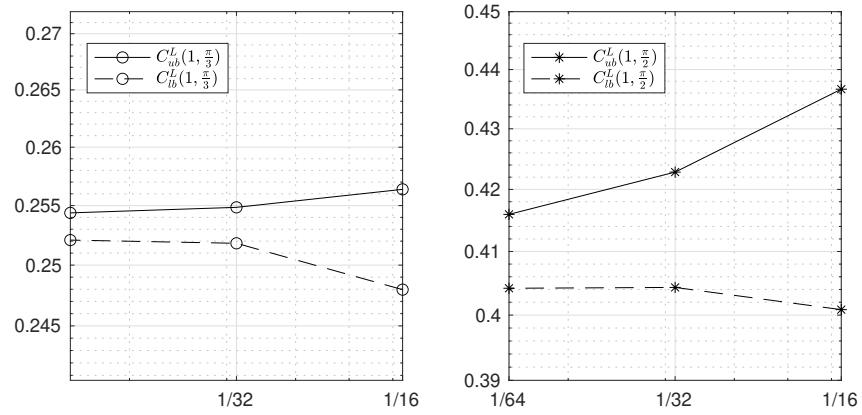


Figure 3.4: The convergency behaviour of the upper and lower bounds of  $C^L(1, \theta)$  for  $\theta = \frac{\pi}{3}$  and  $\frac{\pi}{2}$  ([13]).

# Chapter 4

## Application to partial differential equations

The error estimation extensively discussed in the first three chapters can be used to estimate the finite element solution to certain boundary value problems. In this chapter, such application is discussed.

**The Poisson boundary value problem** Let  $\Omega$  be a convex polyhedral domain in  $\mathbb{R}^2$ , with boundary  $\partial\Omega$ , and consider the second-order boundary value problem for the Poisson equation with Dirichlet boundary conditions:

$$\begin{cases} -\Delta u = f & \text{in } \Omega \\ u = 0 & \text{on } \partial\Omega, \end{cases} \quad (4.1)$$

where  $f \in L^2(\Omega)$  is a given function, assumed to be sufficiently smooth. Under the current setting, the solution  $u$  belongs to  $H^2(\Omega)$ . Also, the relation  $\|\Delta u\|_{0,\Omega} = |u|_{2,\Omega}$  is available.

## 4.1 Local maximum norm error estimation

Let  $\Omega'$  be a subdomain of  $\Omega$  (see Figure 4.1). We aim to propose an *a posteriori* local error estimation for the linear conforming FEM solution  $u_h$  under the maximum error norm. That is,

$$\|u - u_h\|_{\infty,\Omega'} \leq \xi.$$

Here, the explicit value of  $\xi$  will be obtained using two techniques:

1. Maximum norm error estimation for the Lagrange interpolation; and
2. Fujita's method for pointwise estimation of the solution for boundary value problems [12].

The local error estimation is considered through the inequality:

$$\|u - u_h\|_{\infty,\Omega'} \leq \|u - \Pi^L u\|_{\infty,\Omega'} + \|\Pi^L u - u_h\|_{\infty,\Omega'} . \quad (4.2)$$

Here,  $\Pi^L u$  is the Lagrange interpolation of  $u$  over  $\Omega'$ . Let us discuss the estimation of each terms in detail.

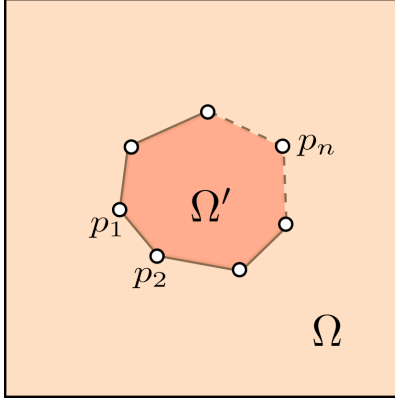


Figure 4.1: The domain  $\Omega$  with the subdomain of interest  $\Omega'$

Estimation of  $\|u - \Pi^L u\|_{\infty, \Omega'}$

Let  $\mathcal{T}_{\Omega'}$  be a triangulation of  $\Omega'$ . Over the triangulation of  $\Omega'$ , define

$$C_h := \max_{K_i} C^L(K_i) . \quad (4.3)$$

Using the results of the optimal estimation for the interpolation error constant for each triangle  $K_i$ , we have

$$\begin{aligned} \|u - \Pi^L u\|_{\infty, \Omega'} &\leq \max_{K_i} C^L(K_i) |u|_{2, K_i} \leq C_h |u|_{2, \Omega} \\ &= C_h \|\Delta u\|_{0, \Omega} = C_h \|f\|_{0, \Omega} . \end{aligned} \quad (4.4)$$

Estimation of  $\|\Pi^L u - u_h\|_{\infty, \Omega'}$

This error term requires a method of pointwise estimation by Fujita [12]. Let  $p_j (j = 1, 2, 3)$  be the vertices of a triangle element  $K$ . For each  $j = 1, 2, 3$ , denote by  $\underline{u}(p_j)$  and  $\bar{u}(p_j)$  the lower bound and upper bound of the pointwise estimate obtained

through Fujita's method in Theorem D.0.1.

Note that  $\Pi^L u - u_h$  is a linear function over element  $K$ . Then,

$$\begin{aligned} \|\Pi^L u - u_h\|_{0,\infty,K} &= \max_{j=1,2,3} |(\Pi^L u - u_h)(p_j)| \\ &\leq \max_{j=1,2,3} \max \{ |(\underline{u} - u_h)(p_j)|, |(\bar{u} - u_h)(p_j)| \} . \end{aligned} \quad (4.5)$$

Thus, for the error term  $\|\Pi^L u - u_h\|_{0,\infty,\Omega'}$ , we apply the above inequality (4.5) to obtain

$$\begin{aligned} \|\Pi^L u - u_h\|_{0,\infty,\Omega'} &= \max_{K_i} \|\Pi^L u - u_h\|_{0,\infty,K_i} \\ &\leq \max_{K_i} \max_{j=1,2,3} \max \left\{ |(\underline{u} - u_h)(p_j^{(i)})|, |(\bar{u} - u_h)(p_j^{(i)})| \right\} , \end{aligned} \quad (4.6)$$

where  $p_j^{(i)}$  ( $j = 1, 2, 3$ ) denote the vertices of triangle  $K_i$ .

**Theorem 4.1.1.** *For the linear conforming FEM solution  $u_h$ , the local error estimation is given by*

$$\|u - u_h\|_{0,\infty,\Omega'} \leq \max_{K_i} \max_{j=1,2,3} \max \left\{ |(\underline{u} - u_h)(p_j^i)|, |(\bar{u} - u_h)(p_j^i)| \right\} + C_h \|f\|_{0,\Omega} . \quad (4.7)$$

*Proof.* From the inequalities (4.4) and (4.6), the conclusion follows.  $\square$

## 4.2 Numerical results and discussion

In this section, we apply the result in Theorem 4.1.1 to a specific boundary value problem.



Consider the boundary value problem (4.1) for  $\Omega = (0, 1)^2$  and  $f$  be taken as  $f(x, y) := 2\pi^2 \sin(\pi x) \sin(\pi y)$ . The linear conforming FEM solution  $u_h$  is obtained through uniform mesh with mesh size  $h_\Omega = 1/80$ .

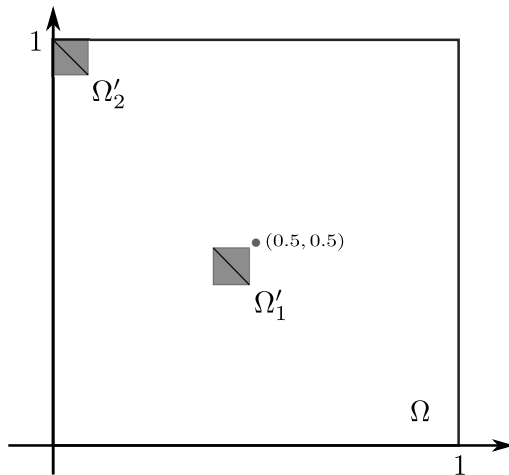


Figure 4.2: Domain  $\Omega$  with two subdomains  $\Omega'_1$  and  $\Omega'_2$

The local error estimation is considered for two subdomains  $\Omega'_1$  and  $\Omega'_2$  in  $\Omega$ . Let  $\Omega'_1$  be formed by the points

$$p_1(0.4375, 0.4375), p_2(0.45, 0.4375), p_3(0.4375, 0.45), p_4(0.45, 0.45),$$

and  $\Omega'_2$  be formed by the points

$$p_1(0, 0.9875), p_2(0.0125, 0.9875), p_3(0, 1), p_4(0.0125, 1).$$

Figure 4.2 shows the domain  $\Omega$  with  $\Omega'_1$  and  $\Omega'_2$ .

Let us first consider the estimation for  $\Omega'_1$ , and apply the same process with  $\Omega'_2$ . Subdivide  $\Omega'_1$  into disjoint right isosceles triangles  $K_1$  and  $K_2$ , where  $K_1$  is formed by

Table 4.1: Approximate pointwise values and explicit bounds obtained using Fujita's method

	$p_1$	$p_2$	$p_3$	$p_4$
upper bound ( $\bar{u}(p_i)$ )	0.9648	0.97143	0.97141	0.9782
approximate	0.9622	0.96896	0.96893	0.97585
lower bound ( $\underline{u}(p_i)$ )	0.9597	0.96648	0.966453	0.97348

$p_1, p_2$ , and  $p_3$ , while  $K_2$  is formed by  $p_2, p_3$ , and  $p_4$ . For each  $i = 1, 2$ , the following terms are estimated:

1.  $\|u - \Pi^L u\|_{\infty, K_i}$ : Note that  $|u|_{2, \Omega} = \|f\|_{0, \Omega} \approx 9.87$ . By symmetry, and using the inequality (3.13) for right isosceles triangles,

$$\|u - \Pi^L u\|_{0, \infty, K_i} \leq 0.41596h \|f\|_{0, 2, \Omega} \approx 0.05132. \quad (4.8)$$

2.  $\|\Pi^L u - u_h\|_{0, \infty, K_i}$ : Next, using Fujita's method, we obtain both the approximate values and the explicit bounds for  $u$  at the vertices  $p_i$ ; see Table 4.1.

Then, by (4.6),

$$\|\Pi^L u - u_h\|_{0, \infty, \Omega'_1} \leq 0.002955. \quad (4.9)$$

Therefore, applying Theorem 4.1.1 and (4.8) and (4.9), we have

$$(0.000485 \approx) \|u - u_h\|_{0, \infty, \Omega'_1} \leq 0.05427.$$

Similarly, applying the same method for  $\Omega'_2$ , we have

$$(0.000385 \approx) \|u - u_h\|_{0,\infty,\Omega'_2} \leq 0.05132 + 0.011172 \approx 0.062492 .$$

*Remark 4.2.1.* It is important to keep in mind the following remarks regarding the proposed local error estimator.

1. Note that, if  $D^2u$  is equally distributed over  $\Omega$ , the term  $|u|_{2,K_i} = O(h)$ , where  $h$  is the mesh size of the triangulation of  $\Omega'$ . Thus, it is expected that  $\|u - \Pi^L u\|_{\infty,\Omega'} = O(h^2)$ . However, since the distribution of  $D^2u$  is not easy to estimate, we utilize  $|u|_{2,K_i} \leq |u|_{2,\Omega}$  in (4.4), which causes a degenerated convergence rate  $O(h)$ .
2. To utilize Fujita's method, it is important that  $\psi_0$  satisfies  $-\operatorname{div} \psi_0 = f$ . In this example, take  $\psi_0 = (\pi \cos(\pi x) \sin(\pi y), \pi \sin(\pi x) \cos(\pi y))$  and indeed

$$-\operatorname{div} \psi_0 = \pi^2 \sin(\pi x) \sin(\pi y) + \pi^2 \sin(\pi x) \sin(\pi y) = f .$$

### 4.2.1 Order of convergence

We investigate the rate of convergence of the local FEM error estimation on  $\Omega'_1$  through different patterns. The difference between the patterns are illustrated below. The term “original mesh” pertains to the uniform triangulation of  $\Omega$  with mesh size  $h$  with which the FEM solution  $u_h$  is obtained.

- (A) FEM solution  $u_h$  obtained over original mesh and  $\Pi^L u$  over  $\Omega'_1$  subdivided into two subtriangles  $K_1$  and  $K_2$ ,

- (B) FEM solution  $u_h$  over the original mesh and  $\Pi^L u$  over once-refined subdivision of  $\Omega'$ ,
- (C) FEM solution  $u_h$  over the original mesh and  $\Pi^L u$  over subdivision of  $\Omega'$  with two times the square of the number of subtriangles as  $\Omega$ .
- (D) FEM solution  $u_{h'}$  over once refined mesh and  $\Pi^L u$  over the same subdivision of  $\Omega'$  as pattern (A)
- (E) FEM solution  $u_{h'}$  over once refined mesh and  $\Pi^L u$  over the same subdivision of  $\Omega'$  as pattern (B)
- (F) FEM solution  $u_{h'}$  over once refined mesh and the  $\Pi^L u$  over subdivision of  $\Omega'$  with two times the square of the number of subtriangles as  $\Omega$ .
- (G) FEM solution  $u_{h'}$  over twice refined mesh and  $\Pi^L u$  over the same subdivision of  $\Omega'$  as pattern (A)
- (H) FEM solution  $u_{h'}$  over twice refined mesh and  $\Pi^L u$  over the same subdivision of  $\Omega'$  as pattern (B)
- (I) FEM solution  $u_{h'}$  over over subdivision of  $\Omega'$  with two times the square of the number of subtriangles as  $\Omega$ .

Let  $h_\Omega (= 1/2)$  be the mesh size of the triangulation of  $\Omega$  used to calculate the FEM solution  $u_h$ , while  $h'_{\Omega'} = |x_2 - x_1|$  be the mesh size of the subdivision of  $\Omega'$  in pattern A. The selection of mesh sizes for each pattern can be confirmed in Table 4.2.

Let  $\xi_F := \|u - u_h\|_{\infty, \Omega'}$ ,  $\xi_L := \|u - \Pi^L u\|_{\infty, \Omega'}$  and their estimates be denoted by  $\tilde{\xi}_F$  and  $\tilde{\xi}_L$ , respectively. By Theorem 4.1.1,  $\tilde{\xi}_F = \tilde{\xi}_L + \xi_{LF}$ , where the error term

Table 4.2: Configurations of meshes

	mesh for $u_h$	mesh for $\Pi^L u$
A	$h_\Omega$	$h'_{\Omega'}$
B	$h_\Omega$	$h'_{\Omega'}/2$
C	$h_\Omega$	$h_{\Omega'} h_\Omega^2$
D	$h_\Omega/2$	$h'_{\Omega'}$
E	$h_\Omega/2$	$h'_{\Omega'}/2$
F	$h_\Omega/2$	$h_{\Omega'} h_\Omega^2/4$
G	$h_\Omega/4$	$h'_{\Omega'}$
H	$h_\Omega/4$	$h'_{\Omega'}/2$
I	$h_\Omega/4$	$h_{\Omega'} h_\Omega^2/16$

$\xi_{LF} := \|\Pi^L u - u_h\|_{\infty, \Omega'_1}$  can be evaluated directly since the involved function has explicit form.

The obtained error terms and relative error for the patterns A-I are displayed in Table 4.3. Table 4.4 on the other hand, shows the relative Lagrange interpolation error for subsequent patterns, where  $r_1$  denotes the actual relative Lagrange interpolation error and  $r_2$  denotes the estimated relative Lagrange interpolation error.

From the numerical computation results, we confirm the following facts.

- The interpolation of  $u$  has the approximation error ( $\xi_L$ ) with convergence rate as  $O(h^2)$  when the triangulation of  $\Omega'$  used for  $\Pi^L u$  is refined from (A) to (B).
- The estimation  $\tilde{\xi}_L$  has a degenerated convergence rate as  $O(h)$ . This is because of the overestimation from the subdomain to the whole domain; see the detail in Remark 4.2.1.

Table 4.3: Error terms involved in the local error estimation

	$\xi_F$	$\tilde{\xi}_L$	$\xi_{LF}$	$\tilde{\xi}_F$	$\frac{ \tilde{\xi}_F - \xi_F }{\xi_F}$
A	0.24971	0.05132	0.25505	0.30637	0.2269
B	0.24971	0.02566	0.25505	0.28071	0.12414
C	0.24971	0.01283	0.25505	0.26788	0.07276
D	0.12872	0.05132	0.00632	0.18287	0.42068
E	0.12872	0.02566	0.13155	0.15721	0.22135
F	0.12872	0.00321	0.13155	0.13476	0.04693
G	0.04674	0.05132	0.04943	0.10075	1.15552
H	0.04674	0.02566	0.04959	0.07525	0.60997
I	0.04674	0.0008	0.04960	0.05040	0.07837

Table 4.4: Relative Lagrange interpolation error

	$\xi_L$	$\tilde{\xi}_L$	$h_{\Omega'}$	$r_1$	$r_2$
A	0.000367	0.05132	$h_{\Omega'}$	-	-
B	0.000091	0.02566	$h_{\Omega'}/2$	4.033	2
C	0.000023	0.01283	$h_{\Omega'}/4$	3.96	2
D	0.00037	0.05132	$h_{\Omega'}$	-	-
E	0.000093	0.02566	$h_{\Omega'}/2$	3.98	2
F	0.0000014	0.00321	$h_{\Omega'}/16$	66.43	7.99
G	0.00039	0.05132	$h_{\Omega'}$	-	-
H	0.000093	0.02566	$h_{\Omega'}/2$	4.19	2
I	0.00000009	0.0008	$h_{\Omega'}/64$	1033.33	32.075

# Chapter 5

## Conclusion

In this research, we provide explicit estimates for the  $L^\infty$ -norm error constant  $C^L(K)$  of the linear Lagrange interpolation function over triangular elements  $K$ . The formula in Theorem 2.3.1 provides a bound of  $C^L$  that holds for triangle of arbitrary shapes. Theorem 3.2.1 in Chapter 3 proposes a numerical approach to obtain optimal bounds for the constant  $C^L$  over a concrete triangle. The optimization problem corresponding to  $C^L$  is novelly solved by utilizing the convex-hull property of Bernstein polynomials.

In addition, we present a method to estimate the local maximum norm of the FEM error of the solution for the boundary value problem of the Poisson equation. For the estimate, we utilized two values: (1) the maximum norm of the Lagrange interpolation error, and (2) the estimate of the maximum difference between the FEM solution and the Lagrange interpolation. To obtain the estimation for the maximum Lagrange interpolation error, the algorithm discussed in Chapter 3 is done for each subtriangle in the subdomain. To estimate the other term, we first use Fujita's

method to obtain approximate and range of the values of the solution  $u$  at the vertices, and then calculate the differences of the FEM solution at the triangulation nodes.

The following problems are left to be explored.

**Relationship between local  $H^2$ -seminorm and global  $H^2$ -seminorm of a function.** In Chapter 4, the maximum norm of the Lagrange interpolation was estimated in terms of  $\|f\|_{0,\Omega}$ , where  $f$  is the function in the boundary value problem of the Poisson equation. This has produced an overestimation in the estimation for the FEM error. In the future, an improved estimate of  $C$  such that  $|u|_{2,\Omega'} \leq C|u|_{2,\Omega}$  for  $\Omega' \subset \Omega$  would benefit the hereby proposed estimate.

**Finite element method with Fujita's pointwise estimation.** Lastly, the pointwise estimation does not utilize the FEM solution  $u_h$  itself and is tediously done at each node of the triangulation. In the future, we aim to extend the method to incorporate pointwise estimation method by Fujita to the FEM solution  $u_h$  and discuss its convergence.



# Appendix A

## Useful inequalities

The following inequalities are fundamental in functional analysis and is beneficial to the study of error estimation.

**Theorem A.0.1.** (Classical Poincaré inequality) *Assume that  $1 \leq p \leq \infty$  and that  $\Omega$  is a bounded open subset of the  $n$ -dimensional Euclidean space  $\mathbb{R}^n$  with a Lipschitz boundary (i.e.,  $\Omega$  is an open, bounded Lipschitz domain). Then there exists a constant  $C$ , depending only on  $\Omega$  and  $p$ , such that for every function  $u$  in the Sobolev space  $W^{1,p}(\Omega)$ ,*

$$\|u - u_\Omega\|_{p,\Omega} \leq C \|\nabla u\|_{p,\Omega}$$

where

$$u_\Omega = \frac{1}{|\Omega|} \int_\Omega u(y) dy$$

is the average value of  $u$  over  $\Omega$ , with  $|\Omega|$  denotes the Lebesgue measure of the domain  $\Omega$ .

**Theorem A.0.2.** (The Friedrichs Inequality) [21] *Let  $G$  be a domain with a Lipschitz*

boundary. Then there exists constants  $c_1, c_2$ , dependent on the considered domain but independent of the functions from  $M$ , such that

$$\int_G u^2(x) dx \leq c_1 \sum_{k=1}^N \int_G \left( \frac{\partial u}{\partial x_k} \right)^2 dx + c_2 \int_{\Gamma} u^2(S) dS$$

holds for every function  $u \in M$ .

For the linear case ( $N = 1$ ), the variations of the Friedrichs inequality are the following:

$$\int_a^b u^2(x) dx \leq c_1 \int_a^b (u')^2(x) dx + c_2 u^2(a), \quad (\text{A.1})$$

$$\int_a^b u^2(x) dx \leq c_1 \int_a^b (u')^2(x) dx + c_2 u^2(b), \quad (\text{A.2})$$

$$\int_a^b u^2(x) dx \leq c_1 \int_a^b (u')^2(x) dx + c_2 [u^2(a) + u^2(b)]. \quad (\text{A.3})$$

To show (A.2), consider

$$g(x) = \cos \frac{\pi(x-a)}{4(b-a)}$$

and  $v = \frac{u}{g}$  or otherwise,  $u = gv$ . Then

$$(u')^2 = (gv)'^2 = (gv' + g'v)^2 = g^2 v'^2 + 2v v' g g' + g'^2 v^2 = g^2 v'^2 + (v^2 g g')' - v^2 g g''$$

holds, so that we have

$$(v^2 g g')' - v^2 g g'' \leq (u')^2 .$$

Then, by integrating over  $[a, b]$ ,

$$[v^2 g g']_a^b - \int_a^b v^2 g g'' dx \leq \int_a^b u'^2 dx .$$

By definition of  $g$ ,

$$g'' = \frac{\pi^2}{16(b-a)^2}g$$

so that

$$v^2 g g'' = \frac{\pi^2}{16(b-a)^2} v^2 g^2 = \frac{\pi^2}{16(b-a)^2} u^2 .$$

Also, note that

$$[v^2 g g']_a^b = \left[ v^2 g^2 \frac{g'}{g} \right]_a^b = \left[ u^2 \frac{g'}{g} \right]_a^b = -\frac{\pi}{4(b-a)} u^2(b)$$

since

$$\frac{g'}{g} = -\frac{\pi}{4(b-a)} \tan\left(\frac{\pi(x-a)}{(b-a)}\right)$$

and in particular

$$\frac{g'(a)}{g(a)} = 0 \quad \frac{g'(b)}{g(b)} = -\frac{\pi}{4(b-a)} .$$

Therefore,

$$\frac{\pi^2}{16(b-a)^2} \int_a^b u^2 dx \leq \int_a^b u'^2 dx + \frac{\pi}{4(b-a)} u^2(b)$$

and

$$\int_a^b u^2 dx \leq \frac{16(b-a)^2}{\pi^2} \int_a^b u'^2 dx + \frac{4(b-a)}{\pi} u^2(b) .$$

Similarly, to show (A.1), we consider

$$g(x) = \cos \frac{\pi(x-b)}{4(b-a)} .$$

To give an improved estimation for (A.3), let us consider

$$g(x) = \sin\left(\frac{\pi(x-a')}{b'-a'}\right)$$

for  $a' = a + \eta$ ,  $b' = b - \eta$ ,  $\eta \geq 0$ . Similar to the above proof, let  $v = \frac{u}{g}$ , or  $u = vg$ .

Then, since

$$g''(x) = \frac{-\pi^2}{(b' - a')^2}g$$

we have

$$v^2 g g'' = \frac{-\pi^2}{(b' - a')^2} v^2 g^2 = \frac{-\pi^2}{(b' - a')^2} u^2 .$$

Also,

$$\begin{aligned} [v^2 g g']_a^b &= \left[ u^2 \frac{g'}{g} \right]_a^b = \frac{\pi}{b' - a'} \left( u^2(b) \cot \left( \frac{\pi(b - a')}{b' - a'} \right) - u^2(a) \cot \left( \frac{\pi(a - a')}{b' - a'} \right) \right) \\ \frac{g'}{g} &= \frac{\pi}{b' - a'} \cot \left( \frac{\pi(x - a')}{b' - a'} \right) \end{aligned}$$

Note that

$$\frac{g'}{g}(a) = \frac{\pi}{b' - a'} \cot \left( \frac{\pi(a - a')}{b' - a'} \right) \quad \frac{g'}{g}(b) = \frac{\pi}{b' - a'} \cot \left( \frac{\pi(b - a')}{b' - a'} \right)$$

Therefore,

$$\int_a^b u^2(x) dx \leq \frac{(b - a + 2\eta)^2}{\pi^2} \int_a^b u'^2(x) dx + \frac{b - a + 2\eta}{\pi} \cot \frac{\pi\eta}{b - a + 2\eta} [u^2(a) + u^2(b)].$$

In addition, if  $u$  satisfies the Dirichlet boundary conditions, that is, if  $u(a) = u(b) = 0$ , then, the following Wirtinger's inequality is obtained.

**Theorem A.0.3.** [10] For any bounded interval  $Q = [a, b]$  and any  $f \in C^1(Q)$  with  $f(a) = f(b) = 0$ ,

$$\int_Q |f|^2 dx \leq \frac{(b - a)^2}{\pi^2} \int_Q |f'|^2 dx .$$

# Appendix B

## Transformation from Bernstein coefficients to Fujino–Morley coefficients

To use the convex-hull property of Bernstein polynomials in Chapter 3, it is necessary to obtain the transformation matrix from Fujino–Morley coefficients to Bernstein coefficients. This chapter shows the method in obtaining the matrix.

Let  $K$  be a reference triangle with vertices  $p_j$ ,  $j = 1, 2, 3$ . The Fujino-Morley basis functions  $\{\phi_i\}_{i=1}^6$  on  $K$  are defined by

$$\phi_i(p_j) = \delta_{i,j}, i, j = 1, 2, 3 \text{ and } \int_{e_i} \frac{\partial \phi_j}{\partial n} \cdot e_i ds = \delta_{i,6-j}, j = 4, 5, 6, i = 1, 2, 3.$$

The Fujino-Morley function space is given by

$$V_h^{FM}(K) := \left\{ u_h \mid \begin{array}{l} u_h|_T \in P_2(T), \forall T \in \mathcal{T}^h; u_h(p_i) = 0, \forall i = 1, 2, 3; u_h \text{ is conti-} \\ \text{nuous on each vertex of } \mathcal{T}^h; \int_e \frac{\partial u_h}{\partial n} ds \text{ is continuous across each} \\ \text{interior edge } e \text{ of } \mathcal{T}^h \end{array} \right\}.$$

For a quadratic function defined on the triangular domain  $K$ , we have

$$f(x, y) = c_1\phi_1 + c_2\phi_2 + \dots + c_6\phi_6 = \sum_{i=1}^6 c_i\phi_i = (\phi_1, \phi_2, \dots, \phi_n) \cdot \begin{pmatrix} c_1 \\ c_2 \\ \vdots \\ c_n \end{pmatrix}. \quad (\text{B.1})$$

On the other hand, for each point  $\mathbf{x} := (x, y) \in K$ , the barycentric coordinates or the area coordinates  $(u, v, w)$  of  $\mathbf{x}$  satisfy

$$\begin{aligned} f(u, v, w) &= \sum_{i+j+k=2} d_{ijk} \binom{2}{ijk} u^i v^j w^k \\ &= d_{200}u^2 + d_{020}v^2 + d_{002}w^2 + 2d_{011}vw + 2d_{101}uw + 2d_{110}uv, \end{aligned}$$

where  $u, v$  and  $w$  are linear in  $K$ .

The Bernstein basis  $\{\psi_j\}_{j=1}^6$  are given by  $\psi_1 = u^2, \psi_2 = v^2, \psi_3 = w^2, \psi_4 = 2vw, \psi_5 = 2uw, \psi_6 = 2uv$  and we rename the constants as  $d_i$  for  $i = 1, 2, \dots, 6$ .

Then, the matrix  $\mathbf{B}$  exists such that

$$\begin{pmatrix} d_1 \\ d_2 \\ \vdots \\ d_n \end{pmatrix} = \mathbf{B} \begin{pmatrix} c_1 \\ c_2 \\ \vdots \\ c_6 \end{pmatrix}, \quad (\text{B.2})$$

that is,  $\mathbf{B}$  is the matrix that transforms the coefficients with respect to the Fujino-Morley basis to the coefficients for the Bernstein basis, which also transforms the Bernstein basis to Fujino-Morley basis.

Then, from (B.1) and (B.2)

$$f = (\phi_1, \phi_2, \dots, \phi_6) \cdot \begin{pmatrix} c_1 \\ c_2 \\ \vdots \\ c_6 \end{pmatrix} = (\psi_1, \psi_2, \dots, \psi_6) \cdot \begin{pmatrix} d_1 \\ d_2 \\ \vdots \\ d_6 \end{pmatrix} = (\psi_1, \psi_2, \dots, \psi_6) \mathbf{B} \cdot \begin{pmatrix} c_1 \\ c_2 \\ \vdots \\ c_6 \end{pmatrix}$$

Thus,  $(\phi_1, \phi_2, \dots, \phi_6) = (\psi_1, \psi_2, \dots, \psi_6) \mathbf{B}$ . We now define the functional  $F_i$  such that  $F_i(\phi_j) = \delta_{i,j}$  for  $i, j = 1, 2, \dots, 6$ .

Now, let  $F = (F_1, F_2, \dots, F_6)$  and define the operation  $\otimes$  through

$$F \otimes (\phi_1, \phi_2, \dots, \phi_6) = \begin{pmatrix} F_1(\phi_1) & \dots & F_1(\phi_6) \\ & \ddots & \\ \vdots & F_i(\phi_j) & \vdots \\ F_6(\phi_1) & \dots & F_6(\phi_6) \end{pmatrix}.$$

Then,  $F \otimes (\phi_1, \phi_2, \dots, \phi_6) = I_{6 \times 6}$ , and  $F \otimes (\psi_1, \psi_2, \dots, \psi_6) \mathbf{B} = I_{6 \times 6}$  which means that

$$\mathbf{B}^{-1} = F \otimes (\psi_1, \psi_2, \dots, \psi_6)$$

where  $B^{-1}$  is the transformation matrix from Fujino-Morley basis to the Bernstein basis. Thus, the component of  $\mathbf{B}^{-1}$  denoted by  $\mathbf{B}_{ij}^{-1}$  is given by

$$\mathbf{B}_{ij}^{-1} = F_i(\psi_j) .$$

**Remark on Barycentric coordinates.** For a triangle  $K$  with vertices  $p_1, p_2, p_3$ , each point  $\mathbf{x}$  in  $K$  corresponds to the area coordinates  $u, v, w$  (see Figure B.1), where

$$u := \frac{|K_1|}{|K|}, \quad v := \frac{|K_2|}{|K|}, \quad w := \frac{|K_3|}{|K|} .$$

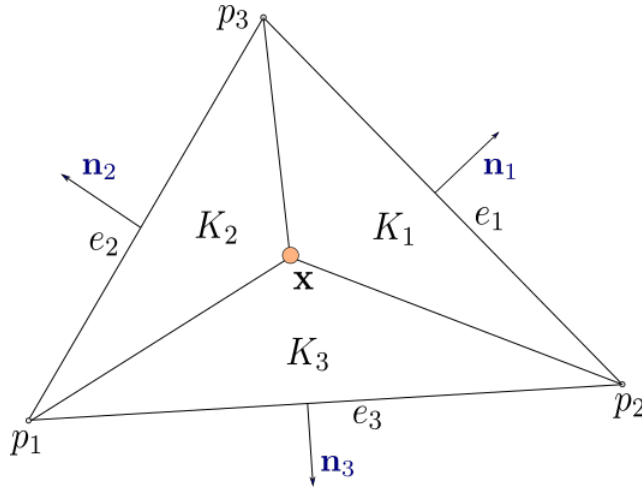


Figure B.1: The subdivision of  $K$  into three subtriangles  $K_1, K_2, K_3$



The integral of the area coordinates in  $K$  is computed through the formula:

$$\int_K u^i(x)v^j(x)w^k(x)dx = \frac{i!j!k!}{(i+j+k+2)!}2|K|.$$

Using the above property, the components of  $\mathbf{B}^{-1}$  are computed as follows.

1. for  $i = 1, 2, 3$  and  $j = 1, 2, \dots, 6$ : Note that  $\psi_i(p_j) = \delta_{ij}$ . Thus,

$$\mathbf{B}_{i,j}^{-1} = F_i(\psi_j) = \psi_j(p_i) = \delta_{i,j}.$$

2. for  $i = 4, 5, 6$ : Note that

$$\mathbf{B}_{i,i-3}^{-1} = F_i(\psi_{i-3}) = \int_{e_{i-3}} \frac{\partial \psi_{i-3}}{\partial n} \cdot e_{i-3} dx = 0$$

since  $\psi_{i-3} = 0$  at  $e_{i-3}$ .

3. for  $i - 3 \neq j$ ,  $i = 4, 5, 6$ ,  $j = 1, 2, 3$ :

$$\mathbf{B}_{i,j}^{-1} = F_i(\psi_j) = \int_{e_{i-3}} \frac{\partial \psi_j}{\partial n} \cdot e_{i-3} dx = \frac{-e_{i-3} \cdot e_j}{2|K|}$$

since  $\psi_j$  is linear on  $e_{i-3}$ .

4. for  $i = 4, 5, 6$ :

$$\mathbf{B}_{i,i}^{-1} = F_i(\psi_j) = \int_{e_{i-3}} \frac{\partial \psi_j}{\partial n} \cdot e_{i-3} dx = \frac{-e_{i-3} \cdot e_{i-3}}{2|K|}$$

5. for  $i \neq j$ ,  $i = 4, 5, 6$ ,  $j = 4, 5, 6$ :

$$\mathbf{B}_{i,j}^{-1} = F_i(\psi_j) = \int_{e_{i-3}} \frac{\partial \psi_j}{\partial n} \cdot e_{i-3} dx = \frac{e_{i-3} \cdot e_{i-3}}{2|K|}$$

# Appendix C

## Algorithm for interpolation error constant estimation

In subsection 3.2.2, the algorithm for optimal estimation of the Lagrange interpolation error constant was discussed. Here, we present the program code to obtain the constant  $C_{ub}^L$  and  $\lambda_h$  in Table 3.2.

```
function [CL,lambda] = myfunc(n, alpha, theta, h_med)
    subdivision_N = 2^(n-1)+1;
    num_nodes = (subdivision_N + 1)*subdivision_N/2;
    num_edges = 3*(subdivision_N)*(subdivision_N-1)/2;
    num_elem = (subdivision_N-1)^2;
    h = h_med/(2^(n-1));
    nodes = 1:num_nodes;
    maxelem = num_nodes + num_edges;
```

```

AREA = alpha*h_med^2*sin(theta)/2;
a_s = AREA/num_elem;
z1 = alpha.*cos(theta);
z2 = alpha.*sin(theta);
Trans = [1 z1; 0 z2];

%%% Defining the node coordinates %%%
node_coordinates_base = zeros(num_nodes,2);
node_index = 0;
for j = 1:subdivision_N
    for i = 1:subdivision_N-j+1
        node_index = node_index+1;
        node_coordinates_base(node_index,:) = [h*(i-1),h*(j-1)];
    end
end
node_coordinates = node_coordinates_base*Trans';

i_start = 0;
N = subdivision_N-1;
edge_labels = num_nodes + 1: num_nodes + num_edges;
edges = [];
for j = 1:N
    for i = 1:N-j+1
        edge = [i, i+1] + i_start;
        edges = [edges; edge];
    end
end

```

```

for i = 1:N-j+1
    edge1 = [i, i+N-j+2] + i_start;
    edge2 = [i+1, i+N-j+2] + i_start;
    edges = [edges; edge1; edge2];
end
i_start = i_start + N-j+2;
end

%%% Definition of triangle elements %%%
node_start = 0;
edge_start = num_nodes;
elements_type1_raw = [];
elements_type2_raw = [];
for j = 1:N
    for i = 1:N-j+1
        edges = [2*i+N-j+1, 2*i+N-j, i] + edge_start;
        nodes = [i, i+1, i+N-j+2] + node_start;
        element = [nodes, edges];
        elements_type1_raw = [elements_type1_raw; element];
    end
    for i = 1:N-j
        edges = [2*i+N-j+1, 2*i+N-j+2, 3*(N-j+1)+i] + edge_start;
        nodes = [i+3+N-j, i+N-j+2, i+1] + node_start;
        element = [nodes, edges];
        elements_type2_raw = [elements_type2_raw; element];
    end
end

```

```

        node_start = node_start + N-j+2;
        edge_start = edge_start + 3*(N-j+1);
    end
    elements = [elements_type1_raw; elements_type2_raw];

%% ASSEMBLY OF THE LOCAL MATRICES %%

E = h*[-1,1;0,-1;1,0];
E = E*Trans';
C = zeros(3,3);
D = zeros(3,3);
for i = 1:3
    for j=1:3
        if i == j
            C(i,j) = 0;
            D(i,j) = dot(E(i,:),E(i,))/(2*a_s);
        else
            C(i,j) = -(dot(E(i,:),E(j,)))/(2*a_s);
            D(i,j) = -dot(E(i,:),E(i,))/(2*a_s);
        end
    end
end

end

%transformation from Fujino-Morley basis to Bernstein basis
Tr_FM2B = [eye(3), zeros(3,3); C D];
%transformation from Bernstein basis to Fujino Morley basis
Tr_B2FM = inv(Tr_FM2B);

```

```

% the local matrix A %
A1 = zeros(3,3);
for i = 1:3
    for j = 1:3
        A1(i,j) = (1/(4*(a_s)^3))*dot(E(i,:),E(j,:))^2;
    end
end
index = [1:3];
A2 = zeros(3,3);
A4 = zeros(3,3);
for i = 1:3
    for j=1:3
        if i == j
            compl1 = setdiff(index,[i]);
            A2(i,j) = (1/(2*(a_s)^3))*(dot(E(i,:),E(compl1(1),:))
            *dot(E(i,:),E(compl1(2),:)));
            A4(i,j) = (1/(2*(a_s)^3))*((dot(E(compl1(1),:),
            E(compl1(1),:))*dot(E(compl1(2),),E(compl1(2),:)))
            +(dot(E(compl1(1),:),E(compl1(2),:))
            *dot(E(compl1(1),:),E(compl1(2),:))));
        else
            compl2 = setdiff(index,[i,j]);
            A2(i,j) = (1/(2*(a_s)^3))*(dot(E(i,:),E(i,:))
            *dot(E(i,:),E(compl2,:)));
            A4(i,j) = (1/(2*(a_s)^3))*((dot(E(compl2,:),E(compl2,:))

```

```

        *dot(E(i,:),E(j,:)))+(dot(E(comp12,:),E(i,:))
        *dot(E(comp12,:),E(j,:))));
    end
end
end
A_bilinearB = [A1 , A2; A2', A4];

% the matrix for the bilinear form of the Fujino Morley basis
% for element type 1 and type 2.
A_bilinearFM_type1 = Tr_B2FM'*A_bilinearB*Tr_B2FM;
A_bilinearFM_type2 = A_bilinearFM_type1;
% global matrix for the bilinear form defined by the
%  $H^2$ -seminorm of the Bernstein basis functions.
tempT = diag([1,1,1,-1,-1,-1]);

%% ASSEMBLY OF THE GLOBAL MATRICES %%

A_global = zeros(maxelem,maxelem);
for i = 1:num_elem
    if elements(i,1) < elements(i,2)
        A_global(elements(i,:),elements(i,:)) += A_bilinearFM_type1;
    else
        A_global(elements(i,:),elements(i,:)) +=
        tempT*A_bilinearFM_type2*tempT;
    end
end
end

```



```

B_global = zeros(6*num_elem,maxelem);
Bvert1 = 1;
Bvert2 = 6*(subdivision_N-2)+2;
Bvert3 = 6*((subdivision_N/2) * (subdivision_N - 1)-1) + 3;
for i = 1:num_elem;
    B_global((i-1)*6+1:6*i,elements(i,:)) = Tr_B2FM;
end
idx = 1:size(A_global,1);
idx([vertex1,vertex2,vertex3])=[];
idxB = 1:size(B_global,1);
idxB([Bvert1,Bvert2,Bvert3])=[];
A = A_global(idx,idx);
B = B_global(idxB,idx);
R = chol(A);
D = (B*inv(A))*B';
[M Idx] = max(diag(D));
lambdax = 1/M;
CL = 1/sqrt(lambdax*(1-(1/2^(n-1))^2));
end

```

# Appendix D

## Fujita's method of pointwise estimation

The method of pointwise estimation of the solution of boundary value problems by Fujita [12] is first presented to bound the values of the Lagrange interpolation function. This method is used in Chapter 4 to estimate the Lagrange interpolation value at the nodes of the triangulation.

**Theorem D.0.1.** [12] *Let  $u_0$  be a vector determined by the equation  $T^*Tu_0 = f$ . For a given vector  $g$  belonging to the range of  $T^*$  we set  $\xi = (u_0, g)_{\mathcal{H}}$ . Let  $u, u', v, v'$  be any vectors satisfying the conditions:*

$$u, u' \in \mathcal{D}, \quad v, v' \in \mathcal{D}^* \quad T^*v = f, \quad T^*v' = g.$$

Then the following inequality holds.

$$\left| \xi - \frac{1}{2}(\alpha + \beta) \right| \leq \frac{1}{2}\epsilon\delta, \quad (\text{D.1})$$

where

$$\alpha = (u, g)_{\mathcal{H}} + (f, u')_{\mathcal{H}} - (Tu, Tu')_{\mathcal{H}'}, \quad \beta = (v, v')_{\mathcal{H}'}, \quad \epsilon = \|Tu - v\|_{\mathcal{H}'}, \quad \delta = \|Tu' - v'\|_{\mathcal{H}'}$$

To apply Theorem D.0.1 for the boundary value problem (4.1), let  $\mathcal{H} = L^2(\Omega)$ ,  $\mathcal{H}' = L^2(\Omega) \times L^2(\Omega)$ , and the operators  $T$  and  $T^*$  be defined as  $Tu := \text{grad } u$ ,  $T^*v := -\text{div } v$ . For pointwise estimation, let  $g$  be the Dirac's delta function singular at a point  $p(x_p, y_p)$ . Then,  $\xi = u_0(p)$ , i.e., the pointwise value of  $u_0$  at  $p$ , where  $u_0$  is the solution for (4.1). In this case, using Theorem D.0.1, the approximate value of  $u_0(p)(= \xi)$  is  $(\alpha + \beta)/2$ .

Set  $r_c = \min\{x_p, y_p, 1 - x_p, 1 - y_p\}$  and consider the following:

$$u_n = \sum_{i=1}^n a_i \varphi_i, \quad v_m = \psi_0 + \sum_{k=1}^m b_k \psi_k, \quad u'_n = \varphi'_0 + \sum_{i=1}^n a'_i \varphi'_i, \quad v'_m = \psi'_0 + \sum_{k=1}^m b'_k \psi'_k$$

where

$$\begin{aligned}
\psi_0 \text{ satisfies } & -\operatorname{div} \psi_0 = f, \\
\psi'_0 = \operatorname{grad} & \left( \frac{1}{2\pi} \log \frac{1}{r} \right) = -\frac{1}{2\pi} \frac{\mathbf{r}}{r^2}, \\
\varphi'_0 = & \begin{cases} \frac{1}{2\pi} \log \frac{1}{r} - \frac{1}{2\pi} \log \frac{1}{r_c} & (r \leq r_c) \\ 0 & (r \geq r_c) \end{cases}, \\
\varphi_n = \varphi'_n = & x^n(x-1)^n y^n (y-1)^n, \quad (n = 1, 2, 3) \\
\psi_n = \psi'_n = & \operatorname{grad} (\operatorname{Re}(z^{4n})), \quad (z = x + iy, n = 1, 2, 3).
\end{aligned}$$

Then, to improve the estimation indicated in Theorem D.0.1, minimize the values of

$$\epsilon^2 = \|Tu_n - v_m\|_{\mathcal{H}'}^2, \quad \delta^2 = \|Tu'_n - v'_m\|_{\mathcal{H}'}^2.$$

*Remark D.0.2.* Generally, it is difficult to find  $\psi_0$  satisfying the condition  $-\operatorname{div} \psi_0 = f$  for an arbitrarily given  $f$ .

# Bibliography

- [1] M. Ainsworth and T. Vejchodský. Robust error bounds for finite element approximation of reaction–diffusion problems with non-constant reaction coefficient in arbitrary space dimension. *Computer Methods in Applied Mechanics and Engineering*, 281:184–199, 2014.
- [2] S. C. Brenner and L. R. Scott. *The Mathematical Theory of Finite Element Methods, 3rd edition*. Springer, New York, 2008.
- [3] R. Burden and J. D. Faires. *Numerical Analysis*. Cengage Learning, 2011.
- [4] W. Cao. On the error of linear interpolation and orientation, aspect ratio and internal angles of a triangle. *SIAM Journal on Numerical Analysis*, 43(1):19–40, 2005.
- [5] C. Carstensen and J. Gedicke. Guaranteed lower bounds for eigenvalues. *Mathematics of Computation*, 83(290):2605–2629, 2014.
- [6] G. Chang and P. J. Davis. The convexity of bernstein polynomials over triangles. *Journal of Approximation Theory*, 40(1):11–28, 1984.

- [7] P. G. Ciarlet. Basic error estimates for elliptic problems. In *Finite Element Methods (Part 1)*, volume 2 of *Handbook of Numerical Analysis*, pages 17–351. Elsevier, Amsterdam, The Netherlands, 1991.
- [8] P. G. Ciarlet. *The Finite Element Method for Elliptic Problems*. Classics in Applied Mathematics. Society for Industrial and Applied Mathematics, Philadelphia, PA, 2002.
- [9] E. F. D’Azevedo and R. B. Simpson. On optimal interpolation triangle incidences. *SIAM Journal on Scientific and Statistical Computing*, 10(6):1063–1075, 1989.
- [10] H. Dym and H. P. McKean. *Fourier series and integrals [by] H. Dym [and] H. P. McKean*. Academic Press New York, 1972.
- [11] R. T. Farouki. The bernstein polynomial basis: A centennial retrospective. *Computer Aided Geometric Design*, 29(6):379–419, 2012.
- [12] H. Fujita. Contribution to the theory of upper and lower bounds in boundary value problems. *Journal of the Physical Society of Japan*, 10(1):1–8, 1955.
- [13] S. M. Galindo, K. Ike and X. Liu. Error-constant estimation under the maximum norm for linear lagrange interpolation. *Journal of Inequalities and Applications*, 2022(1):109, 2022.
- [14] F. Kikuchi and X. Liu. Estimation of interpolation error constants for the p0 and p1 triangular finite elements. *Computer methods in applied mechanics and engineering*, 196(37-40):3750–3758, 2007.
- [15] K. Kobayashi. On the interpolation constants over triangular elements. *RIMS Kokyuroku*, 1733:58–77, 2010.

- [16] X. Liu. Ganjin online computing platform. <http://ganjin.online>.
- [17] X. Liu. A framework of verified eigenvalue bounds for self-adjoint differential operators. *Applied Mathematics and Computation*, 267:341–355, 2015.
- [18] X. Liu and F. Kikuchi. Analysis and estimation of error constants for  $P_0$  and  $P_1$  interpolations over triangular finite elements. *Journal of Mathematical Sciences, the University of Tokyo*, 17(1):27–78, 2010.
- [19] X. Liu and S. Oishi. Verified eigenvalue evaluation for the laplacian over polygonal domains of arbitrary shape. *SIAM Journal on Numerical Analysis*, 51(3):1634–1654, 2013.
- [20] X. Liu and C. You. Explicit bound for quadratic lagrange interpolation constant on triangular finite elements. *Applied Mathematics and Computation*, 319(1):693–701, 2018.
- [21] K. Rektorys. *Variational Methods in Mathematics, Science and Engineering*. Springer Netherlands, 2012.
- [22] J. Shewchuk. What is a good linear finite element? interpolation, conditioning, anisotropy, and quality measures. In *Invited Talk, 11th International Meshing Roundtable*, pages 115–126, New York, NY, 2002. Springer-Verlag.
- [23] S. Liao, Y. Shu and X. Liu. Optimal estimation for the fujino–morley interpolation error constants. *Japan Journal of Industrial and Applied Mathematics*, 36:521–542, 2019.
- [24] S. Waldron. The error in linear interpolation at the vertices of a simplex. *SIAM Journal on Numerical Analysis*, 35(3):1191–1200, 1998.

- [25] C. You, H. Xie and X. Liu. Guaranteed eigenvalue bounds for the steklov eigenvalue problem. *SIAM Journal on Numerical Analysis*, 57(3):1395–1410, 2019.